AMERICAN SOCIETY FOR MICROBIOLOGY | Journal of Virology®

VACCINES AND ANTIVIRAL AGENTS

A Derivative of the D5 Monoclonal Antibody That Targets the gp41 N-Heptad Repeat of HIV-1 with Broad Tier-2-Neutralizing Activity

Adonis A. Rubio,[a,b] Maria V. Filsinger Interrante,[a,c,d] Benjamin N. Bell,[a,e] Clayton L. Brown,[a,f] Theodora U. J. Bruun,[a,f] Celia C. LaBranche,[g,h] David C. Montefiori,[g,h] Peter S. Kim[a,f,i]

[a]Stanford ChEM-H, Stanford University, Stanford, California, USA
[b]Department of Biology, Stanford University School of Humanities & Sciences, Stanford, California, USA
[c]Stanford Biophysics Program, Stanford University School of Medicine, Stanford, California, USA
[d]Stanford Medical Scientist Training Program, Stanford University School of Medicine, Stanford, California, USA
[e]Department of Molecular and Cellular Physiology, Stanford University School of Medicine, Stanford, California, USA
[f]Department of Biochemistry, Stanford University School of Medicine, Stanford, California, USA
[g]Department of Surgery, Duke University Medical Center, Durham, North Carolina, USA
[h]Duke Human Vaccine Institute, Duke University Medical Center, Durham, North Carolina, USA
[i]Chan Zuckerberg Biohub, San Francisco, California, USA

ABSTRACT HIV-1 infection is initiated by the viral glycoprotein Env, which, after interaction with cellular coreceptors, adopts a transient conformation known as the prehairpin intermediate (PHI). The N-heptad repeat (NHR) is a highly conserved region of gp41 exposed in the PHI; it is the target of the FDA-approved drug enfuvirtide and of neutralizing monoclonal antibodies (mAbs). However, to date, these mAbs have only been weakly effective against tier-1 HIV-1 strains, which are most sensitive to neutralizing antibodies. Here, we engineered and tested 11 IgG variants of D5, an anti-NHR mAb, by recombining previously described mutations in four of D5's six antibody complementarity-determining regions. One variant, D5_AR, demonstrated 6-fold enhancement in the 50% inhibitory dose (ID_{50}) against lentivirus pseudotyped with HXB2 Env. D5_AR exhibited weak cross-clade neutralizing activity against a diverse set of tier-2 HIV-1 viruses, which are less sensitive to neutralizing antibodies than tier-1 viruses and are the target of current antibody-based vaccine efforts. In addition, the neutralization potency of D5_AR IgG was greatly enhanced in target cells expressing FcγRI, with ID_{50} values of <0.1 μg/ml; this immunoglobulin receptor is expressed on macrophages and dendritic cells, which are implicated in the early stages of HIV-1 infection of mucosal surfaces. D5 and D5_AR have equivalent neutralization potency in IgG, Fab, and single-chain variable-fragment (scFv) formats, indicating that neutralization is not impacted by steric hindrance. Taken together, these results provide support for vaccine strategies that target the PHI by eliciting antibodies against the gp41 NHR and support investigation of anti-NHR mAbs in nonhuman primate passive immunization studies.

IMPORTANCE Despite advances in antiretroviral therapy, HIV remains a global epidemic and has claimed more than 32 million lives. Accordingly, developing an effective HIV vaccine remains an urgent public health need. The gp41 N-heptad repeat (NHR) of the HIV-1 prehairpin intermediate (PHI) is highly conserved (>90%) and is inhibited by the FDA-approved drug enfuvirtide, making it an attractive vaccine target. However, to date, anti-NHR antibodies have not been potent. Here, we engineered D5_AR, a more potent variant of the anti-NHR antibody D5, and established its ability to inhibit HIV-1 strains that are more difficult to neutralize and are more representative of circulating strains (tier-2 strains). The neutralizing activity of D5_AR

Citation Rubio AA, Filsinger Interrante MV, Bell BN, Brown CL, Bruun TUJ, LaBranche CC, Montefiori DC, Kim PS. 2021. A derivative of the D5 monoclonal antibody that targets the gp41 N-heptad repeat of HIV-1 with broad tier-2-neutralizing activity. J Virol 95:e02350-20. https://doi.org/10.1128/JVI.02350-20.

Editor Frank Kirchhoff, Ulm University Medical Center

Address correspondence to Peter S. Kim, kimpeter@stanford.edu.

Received 9 December 2020
Accepted 30 April 2021
Accepted manuscript posted online 12 May 2021
Published 12 July 2021

was greatly potentiated in cells expressing FcγRI; FcγRI is expressed on cells that are implicated at the earliest stages of sexual HIV-1 transmission. Taken together, these results bolster efforts to target the gp41 NHR and the PHI for vaccine development.

KEYWORDS HIV-1, antibodies, prehairpin intermediate, virus

More than 35 million people currently live with HIV/AIDS globally (https://www.who.int/news-room/fact-sheets/detail/hiv-aids); despite the promise of antiretroviral therapy, a preventative HIV-1 vaccine remains an urgent global health need. However, after more than three decades of intense research, a prophylactic HIV/AIDS vaccine remains elusive. The RV144 trial raised expectations in 2009 (1), but the lack of efficacy reported in 2020 for the HVTN702 trial in South Africa, which was based on the prime-boost regimen utilized in RV144, was another major setback for the field (2).

Many current HIV-1 vaccine-directed research efforts are motivated by the finding that rare broadly neutralizing antibodies (bNAbs) can be isolated from patients chronically infected with HIV-1 (3–22). The main epitopes of these bNAbs include the CD4 binding site (CD4bs), the membrane proximal external region (MPER), the V1/V2 region, and the V3 glycan (23–26). Importantly, bNAbs are generally elicited as a result of complex coevolutionary pathways with viral variants and thus tend to be characterized by extensive somatic hypermutation (SHM) of the antibody genes. Indeed, germline precursors of bNAbs typically do not bind to most Env proteins (7, 27, 28). As a result, germline-lineage approaches (5, 10, 12, 15, 16, 21, 22) have emerged wherein an engineered immunogen is used to stimulate a germline precursor of a bNAb, followed by multistage multicomponent immunization aimed to direct affinity maturation toward the desired bNAb. While some progress has been made in eliciting bNAb-like responses in nonhuman primates (NHPs) (29–31), the technical and biological difficulties in eliciting rare bNAbs represent critical barriers to developing an antibody-based HIV vaccine against the native prefusion conformation of Env.

In contrast to these bNAb epitopes on the native conformation of Env, one highly conserved region of HIV-1 gp41 is exposed in a transient form of Env that is critical for viral infection, the prehairpin intermediate (PHI). Upon binding cellular receptors, Env undergoes substantial conformational changes to form the PHI, in which the N-heptad repeat (NHR) and C-heptad repeat (CHR) regions are exposed before the cellular and viral membranes come together for membrane fusion (32–34). Due to its high sequence conservation (~93%) (https://www.hiv.lanl.gov/content/sequence/HIV/mainpage.html) and critical role in viral entry (32), the NHR is a promising target for blocking HIV-1 infection. Several inhibitors of HIV-1 infection that target the NHR and prevent viral membrane fusion have been identified (35–48). Cyclic D-peptide inhibitors that target the NHR have been used to prevent and treat simian-human immunodeficiency virus (SHIV) infection in rhesus macaques (35, 49). Most notably, the FDA-approved HIV-1 fusion inhibitor enfuvirtide (50–52) validates the NHR as a therapeutic target in humans.

Of relevance for vaccine applications, several monoclonal antibodies (mAbs) that target the NHR and inhibit HIV-1 infection have been characterized (53–57). The first of these mAbs was D5 (53), which was isolated from a human B cell-derived phage display library using two synthetic mimetics of the gp41 PHI: 5-helix (36) and IZN36 (58). X-ray crystallographic studies reveal that D5 binds a conserved hydrophobic pocket of the NHR (59). In contrast to most HIV-1 bNAbs (9, 60–66), D5 and other neutralizing mAbs that target the NHR (53–56, 67) contain far fewer amino acid changes resulting from SHM (Fig. 1). Thus, eliciting anti-PHI antibodies via vaccination is not expected to require extensive germline-targeting strategies. Indeed, various NHR-based vaccine candidates have been shown to elicit HIV-1-neutralizing antisera in animals (56, 68–70). These antisera, however, demonstrate only weak neutralization potency. Similarly, while exhibiting broad neutralizing activity, the potencies of mAbs targeting the NHR, including D5, are weak and mostly limited to tier-1 HIV-1 isolates (53–56). Taken

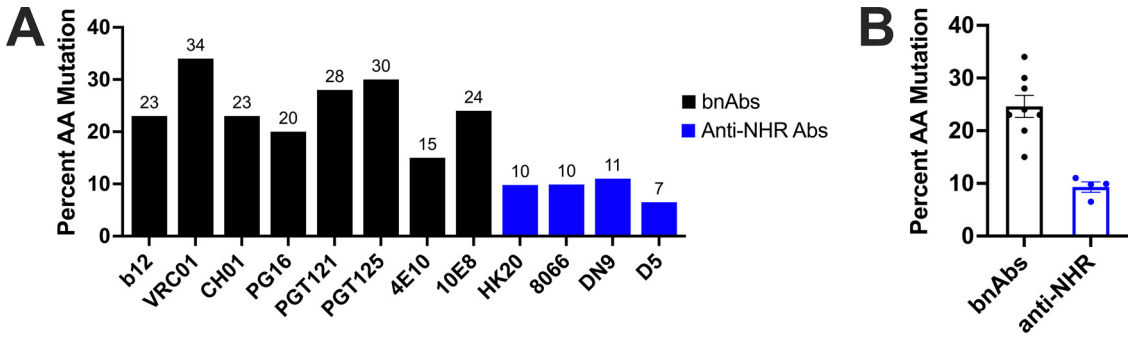

FIG 1 Anti-NHR antibodies have a lower level of somatic hypermutation than HIV-1 bNAbs. (A) Percentages of mutated amino acids across both heavy- and light-chain V genes from germline are reported for eight bNAbs (black) representative of the four main bNAb epitopes (MPER, V1/V2 region, V3 glycan, and CD4bs) and four monoclonal antibodies against the NHR (blue). Sequences of the antibodies involved in this analysis were previously reported (17, 54–56, 60–67). This analysis included the full sequence of the framework regions 1, 2, and 3 and CDR1 and −2. (B) Comparison of percent amino acid mutation between bNAbs (using the eight bNAbs presented in panel A) and anti-NHR antibodies; bNAbs have a mean somatic hypermutation of 25% compared to the 9.5% for anti-NHR antibodies. Each dot represents a unique antibody's percent amino acid mutation, with error bars denoting standard errors of the means. The percentages of amino acid mutations from germline are reported on the *y* axis, as the published sequences cited above mostly reported only amino acid sequences.

together, these findings have led to understandable skepticism about the PHI as a vaccine target.

Here, we engineered more-potent versions of D5 by combining multiple mutations in the complementarity-determining region (CDR) loops of the antibody that were individually shown to increase the neutralization activity of D5 by Montgomery et al. (67). The most enhanced recombined variant, D5_AR, shows neutralization efficacy in several diverse tier-2 HIV-1 viruses. Thus, D5_AR presents proof of concept that an anti-PHI mAb, with low levels of SHM, can neutralize tier-2 HIV-1 viruses. In addition, as recently reported for D5 (71) and earlier for MPER mAbs (72, 73), the neutralization potency of D5_AR was enhanced ~1,000-fold in target cells expressing the high-affinity immunoglobulin receptor FcγRI compared to those without. These results bolster attempts to target the PHI as an alternative and orthogonal approach toward an HIV-1 vaccine that is fundamentally different from the prevalent germline-targeting strategies to elicit bNAbs.

RESULTS

D5_AR, a recombined CDR mutant of D5, has enhanced neutralization potency against HIV-1 *in vitro*. X-ray crystallography revealed that complementarity-determining region (CDR) loops in the antibody variable regions of both the heavy and light chains (VH and VL, respectively) contribute to the binding of D5 to the NHR (59). Informed by this insight, Montgomery et al. (67) sought to increase the neutralization potency of D5 by randomizing residues in five of the six CDRs (VH CDR1, −2, and −3 and VL CDR1 and −3). Four D5 IgG variants, each with only one CDR mutated, had slightly increased neutralization potency (67).

To assess the impact on neutralization after the introduction of multiple mutated CDRs, we recombinantly expressed and purified wild-type D5 IgG and 15 D5 IgG variants (Fig. 2). The variants were designated D5_HXXX_LX (Fig. 2C), with each X replaced by either 0 (representing the wild-type sequence) or 1 (representing the mutated CDR sequence) in the heavy (CDR1, −2, and −3) or light (CDR3) chain (Fig. 2A), reported by Montgomery et al. (67). These four CDRs form critical points of contact at the D5 epitope of the NHR (Fig. 2B). Using single-round infectivity assays in TZM-bl cells, each D5 IgG variant was screened for neutralization potency against lentivirus pseudotyped with HIV-1 HXB2 Env (74–78). Neutralization potency was reported as the 50% inhibitory dose (ID_{50}). We confirmed that the four single-CDR mutants previously described by Montgomery et al. (67) (D5_H100_L0, D5_H010_L0, D5_H001_L0, and D5_H000_L1) displayed enhanced neutralization versus the parent D5.

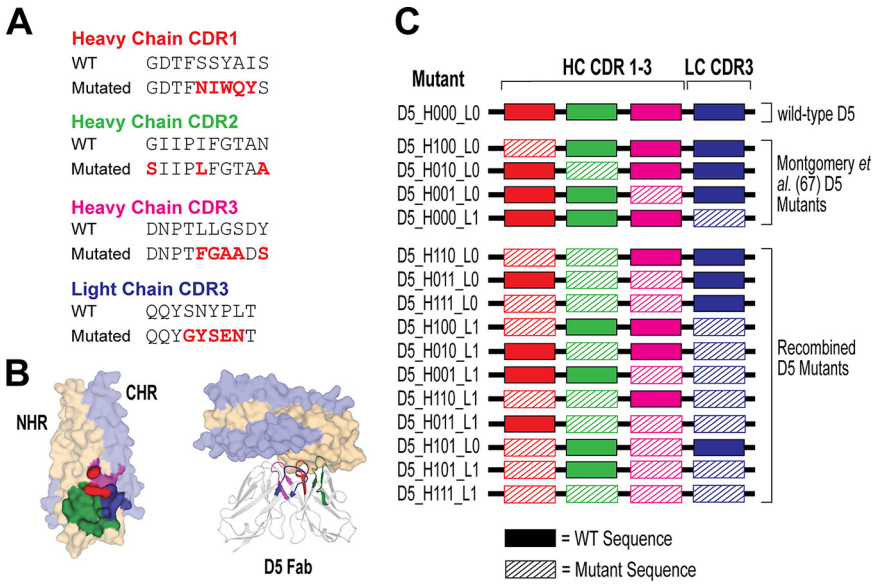

FIG 2 Recombination of known beneficial CDR sequences to engineer novel D5 variants. (A) Mutated CDR sequences of four highlighted D5 variants reported by Montgomery et al. (67) aligned with the wild-type (WT) sequence. These mutated CDR sequences were used to engineer the 11 recombined variants. (B) Left, paratope map of the binding sites for D5 Fab with its antigen, 5-helix. NHR, yellow; CHR, light blue. Areas of contact with the D5 CDR loops are represented as VH CDR1 (red), VH CDR2 (green), VH CDR3 (magenta), and VL CDR3 (blue). Right, X-ray crystal structure of D5 in complex with 5-helix (PDB 2CMR) (59). (C) Schematic of D5 variants engineered and tested. The identity of each of the four CDR loops is represented by 0 (WT) or 1 (mutant).

Next, we screened 11 additional D5 variants with lentivirus pseudotyped with HIV-1 HXB2 Env for neutralization potency using a single-round infectivity assay. Several recombinant D5 variants had little effect or even diminished the neutralization potency compared to that of D5 (Table 1). Nevertheless, we identified six D5 variants that modestly enhanced (>2.0-fold) the neutralization potency of D5 (Table 1). Among these, D5_H011_L0, in which both CDR2 and CDR3 of the heavy chain are mutated, demonstrated the greatest enhancement (4-fold) in ID_{50} (Table 1). We renamed this enhanced D5 variant D5_AR.

To further characterize D5_AR, we assessed the difference in binding for D5_AR Fab compared to D5 Fab against CCIZN17, a variation of a previously described mimetic of the NHR trimer (58, 79), using biolayer interferometry (see Materials and Methods). The Fab for D5_AR has ~38-fold higher affinity for CCIZN17 than for D5 (1.6 nM for D5_AR compared to 61 nM for D5), providing a potential explanation for the enhanced neutralization activity of D5_AR (Fig. 3).

Size exclusion chromatography purification impacts D5's neutralization potency. Our initial neutralization screen (Table 1) utilized antibody purified via protein A affinity chromatography (see Materials and Methods). To obtain a more in-depth neutralization profile for D5_AR compared to that of D5, which included testing the constructs' neutralization potency against various viruses and in different antibody formats, we added a size exclusion chromatography (SEC) step following protein A affinity chromatography. Notably, we found that the manner of purification of antibodies impacted the observed neutralization activity of the antibody (Fig. 4). A side-by-side comparison of a D5_AR antibody prep that was purified via only protein A chromatography with D5_AR that had the subsequent SEC purification step revealed that there was indeed a difference in neutralization for D5_AR (Fig. 4C); however, neutralization was still enhanced compared to that of D5. Reviewing the UV traces from SEC performed after affinity chromatography, we observed and removed aggregates for both D5 and D5_AR IgG (Fig. 4A and B). We note that the aggregate fraction in the SEC traces (Fig. 4A and B) accounted for 8.2% and 11% of the total protein for D5 and

TABLE 1 Neutralization profiles of D5 variants

Profile	D5 IgG variant	ID_{50} (μg/ml)[a]	Fold change[b]	*n*
Wild-Type	D5	48 ± 4.2	1.0	18
Modestly enhanced (>2.0-fold)	D5_H011_L0 (D5_AR)	12 ± 2.2	4.0 ± 0.78	6
	D5_H110_L0	20 ± 1.9	2.7 ± 0.57	4
	D5_H101_L0	20 ± 8.3	2.7 ± 0.34	3
	D5_H100_L0	31 ± 9.5	2.5 ± 0.84	2
	D5_H010_L0	35 ± 4.8	2.5 ± 0.12	2
	D5_H000_L1	33 ± 2.5	2.3 ± 0.78	2
Little to no effect (1.0- to 2.0-fold)	D5_H010_L1	42 ± 2.3	2.0 ± 0.79	3
	D5_H111_L0	43 ± 9.2	1.9 ± 0.41	4
	D5_H001_L0	54 ± 12	1.8 ± 0.36	2
	D5_H111_L1	62 ± 4.5	1.7 ± 0.68	3
	D5_H110_L1	28 ± 0.07	1.4 ± 0.03	2
	D5_H011_L1	80 ± 4.3	1.0 ± 0.06	2
Diminished neutralization (<1.0-fold)	D5_H100_L1	100 ± 9.8	0.47 ± 0.07	2
	D5_H101_L1	>300	NA	2
	D5_H001_L1	>300	NA	3

[a]The ID_{50} (half maximal inhibitory dose) of each D5 variant is represented by the geometric mean and standard error of the mean from replicate experiments.

[b]For each infection assay, the fold enhancement versus D5 was calculated ($ID_{50,\ D5}/ID_{50,\ D5\ variant}$); reported fold enhancement is the geometric mean and standard error from replicate experiments. Fold enhancement of >1 corresponds to enhanced neutralization potency (reduced ID_{50}). NA, not applicable.

D5_AR, respectively; this is in comparison to the 90% and 83% in the major IgG fraction for D5 and D5_AR, respectively. We hypothesize that the presence of aggregates reduced the neutralization potencies of D5 and D5_AR, possibly because aggregated D5 has less neutralizing activity. Once aggregates were removed, D5 and D5_AR IgG preparations did not form aggregates readily. SEC-purified D5_AR samples frozen in 10% glycerol-1× phosphate-buffered saline (PBS) solution at −20°C retain similar neutralization activity after thawing (Fig. 4D).

Experiments in Table 1 were the only experiments reported here that used non-SEC-purified antibody preparations, which accounts for the difference in ID_{50} values for HXB2 reported in Table 1 (and see Fig. 6) (SEC-purified preparations had a 1.5-fold decrease in ID_{50} for D5 and a 2.3-fold decrease in ID_{50} for D5_AR).

D5 and D5_AR neutralize with similar potency as an scFv, Fab, and IgG. In the first description of D5, the IgG (~150 kDa) and single-chain variable-fragment (scFv) (~25 kDa) constructs neutralized similarly to one another (53). However, more recent studies reported that D5 scFv is more potent than D5 Fab (~50 kDa) and that both were more potent than D5 IgG (59, 67, 80); in addition, there are reports that increasing the size of NHR inhibitors reduces neutralization potency (55, 67, 80–82). These size-dependent findings would imply steric hindrance in accessing the PHI. Given our finding that SEC purification impacted the neutralization potency of D5 and D5_AR IgG (Fig.

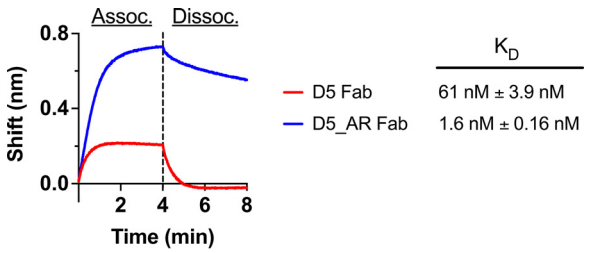

FIG 3 D5_AR Fab has a greater binding affinity to CCIZN17, an NHR-mimetic, than D5 Fab. The binding affinity (reported numerically as the K_D) of D5 (red) and D5_AR (blue) Fab for CCIZN17, a variation of a previously described NHR mimetic (58, 79), is presented as association and dissociation curves using biolayer interferometry. The K_Ds are reported as the means from fitted values across multiple concentrations from at least two independent experiments and are reported with the standard errors of the means.

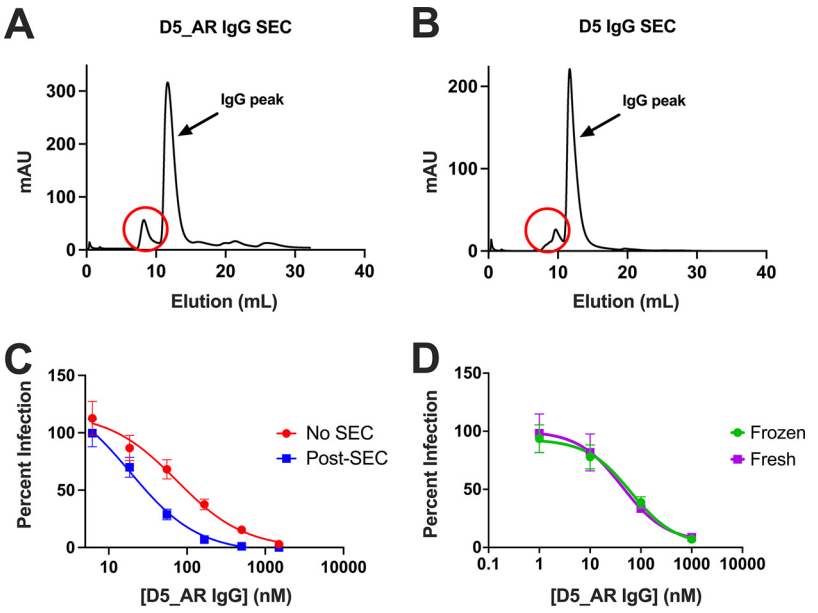

FIG 4 Purification via size exclusion chromatography (SEC) impacts the neutralization potency of D5_AR and reveals possible aggregation. (A and B) UV traces from SEC, performed after affinity chromatography, reveal possible protein aggregates (circled in red) for both D5 and D5_AR IgG. (A) The potential aggregate peak for D5_AR accounts for 11% of the total protein, while the major IgG fraction accounts for 83%. (B) Similarly, the aggregate fraction for D5 accounts for 8.2% of the total protein compared to the 90% of the major D5 IgG fraction. (C) After SEC purification, D5_AR IgG preparations demonstrated enhanced neutralization activity compared to that of a prep that was only purified via affinity chromatography. Each data point represents the mean percent infection with standard error of the mean ($n = 3$). (D) SEC-purified D5_AR IgG sample preps stored in 10% glycerol-1× PBS solution at −20°C retained similar neutralization activity after being thawed. Each data point represents the mean percent infection with standard error of the mean ($n = 3$).

4C), we decided to reinvestigate the question of size-dependent neutralization for D5 using antibody preparations free of aggregates. Notably, in agreement with the initial report (53) and in contrast to other reports (59, 67, 80), we found that D5 as an IgG, Fab, and scFv (all SEC purified) did not exhibit a size-dependent pattern of neutralization (Fig. 5A). This difference may be due to our final size exclusion chromatography step, which, to our knowledge, was not performed in other studies in which size dependence was observed. Additionally, we detected comparable neutralization potency for D5_AR as an scFv, Fab, and IgG (Fig. 5B). These results demonstrate that neither D5 nor D5_AR is impacted by steric hindrance and suggest the presence of protein aggregates could explain previous reports of size-dependent neutralization for D5 scFv, Fab, and IgG.

D5_AR exhibits cross-clade tier-2 neutralization of HIV-1 viruses. We next investigated the potency of D5_AR IgG in neutralizing a diverse panel of 19 tier-1 and tier-2 pseudotyped viruses across eight viral clades (A, AC, B, C, G, CRF01, CRF02, and CRF07) (77, 83–98). Ten of these strains originated from a 12-virus panel designed to capture the sequence diversity of the HIV-1 epidemic globally (77). Tier-1A and tier-1B contain viruses that are most sensitive to neutralization by antibodies, whereas tier-2 viruses have modest sensitivity to neutralizing antibodies (90). D5_AR IgG neutralized virus more effectively than D5 IgG across all tiers and clades (Fig. 6A). Notably, D5_AR neutralized more viruses with an ID_{50} of $<50\,\mu$g/ml (63%) than D5 (11%) (Fig. 6B).

D5_AR neutralization potency is enhanced >1,000-fold in FcγRI-expressing cells. Recently, we reported the neutralization potency of D5 IgG to be greatly increased in TZM-bl cells expressing the cell surface receptor FcγRI (TZM-bl/FcγRI cells) (71). FcγRI is the only known IgG receptor in humans capable of binding monomeric IgG with high affinity (99). To determine whether D5_AR IgG is similarly potentiated, we tested its neutralization of an additional panel of tier-2 HIV-1 viruses and SHIV

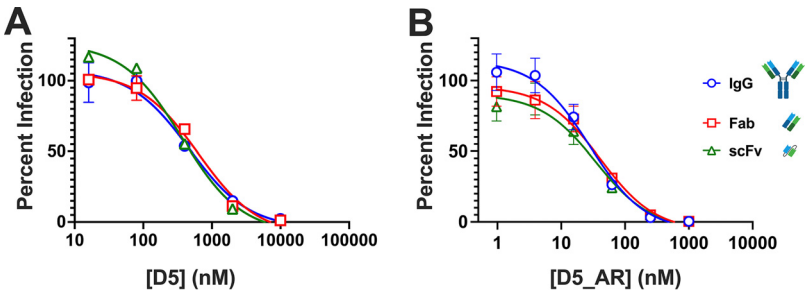

FIG 5 D5 and D5_AR neutralize HIV-1 *in vitro* in a size-independent manner. scFv, Fab, and IgG constructs of D5 (A) and D5_AR (B) are similarly effective *in vitro* at neutralizing lentivirus pseudotyped with HIV-1 HXB2. Data points and error bars are the mean percent infections and standard errors of the means, respectively ($n = 2$). Antibody construct images used in this figure were generated with BioRender.

challenge viruses in TZM-bl/FcγRI cells (Fig. 7). As recently reported for D5 (71), and as previously characterized for MPER mAbs (72, 73), the neutralization potency of D5_AR was enhanced at least 1,000-fold in TZM-bl/FcγRI cells compared to that in TZM-bl cells without FcγRI (Fig. 7A and B). In the presence of FcγRI, D5_AR had potent neutralization activity against a panel of tier-2 HIV-1 viruses, with ID_{50} values of $<0.1\,\mu g/ml$ (Fig. 7C and D). Consistent with an Fc-dependent mechanism, the Fab form of D5_AR did not

A

Env Pseudotype	Tier	Clade	ID_{50} (μg/mL)		*n*
			D5	D5_AR	(D5, D5_AR)
SF162	1A	B	120 ± 81	42 ± 17	(2,2)
MW965	1A	C	9.8 ± 3.6	2.5 ± 0.041	(2,2)
Q23	1B	A	90 ± 4.8	26 ± 8.4	(2,2)
92RW020.5	1B	A	180 ± 42	21 ± 14	(2,2)
X2278	1B	B	130 ± 36	9.4 ± 4.1	(2,4)
HXB2	1B	B	31 ± 5.5	5.3 ± 1.2	(5,13)
BaL	1B	B	>200	26 ± 8.3	(3,2)
SS1196	1B	B	130 ± 46	23 ± 12	(2,2)
ZM197M.PB7	1B	C	140 ± 66	52 ± 28	(2,2)
DJ263.8	1B	CRF02	>200	45 ± 13	(2,2)
246-F3	2	AC	>200	140 ± 27	(2,2)
TRO.11	2	B	180 ± 1.4	54 ± 14	(2,3)
25710	2	C	200 ± 4.1	22 ± 11	(2,3)
Ce1176	2	C	>200	140 ± 23	(2,2)
Ce0217	2	C	180 ± 11	85 ± 28	(2,3)
CNE55	2	CRF01	>200	89 ± 32	(2,3)
BJOX2000	2	CRF07	>200	46 ± 5.5	(2,3)
CH119	2	CRF07	>200	40 ± 28	(2,4)
X1632	2	G	>200	66 ± 7.8	(2,3)

B

FIG 6 D5_AR IgG has higher neutralization potency than D5 across tiers and clades of HIV-1. (A) D5_AR IgG has an enhanced neutralization profile versus D5 IgG, as indicated by ID_{50} values (geometric mean ± standard error of the mean) against a panel of tier-1 and tier-2 HIV-1 viruses from multiple clades. (B) D5_AR IgG neutralizes a greater percentage of HIV-1 viruses than D5 IgG within the $<10\,\mu g/ml$ and 10 to $50\,\mu g/ml$ ID_{50} ranges.

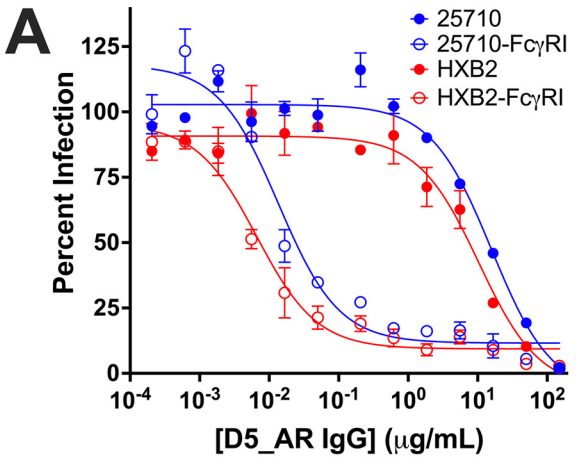

B

Virus	TZM-bl	TZM-bl/FcγRI	Fold Enhancement
HXB2	10 μg/mL	0.0066 μg/mL	1500
25710	16 μg/mL	0.014 μg/mL	1100

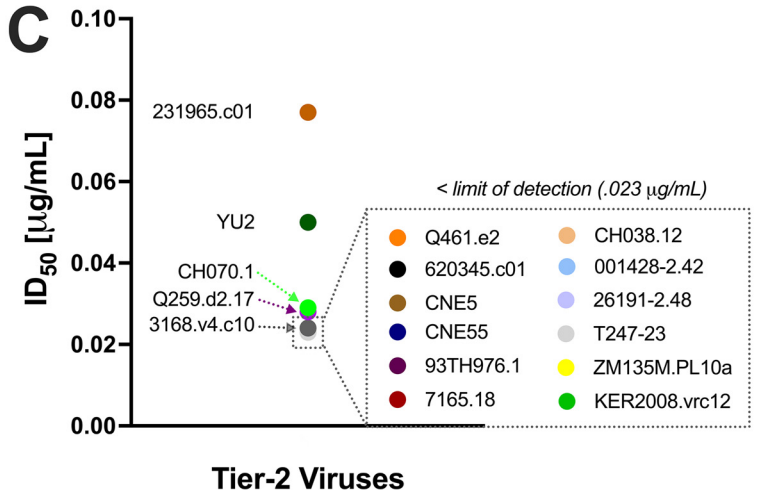

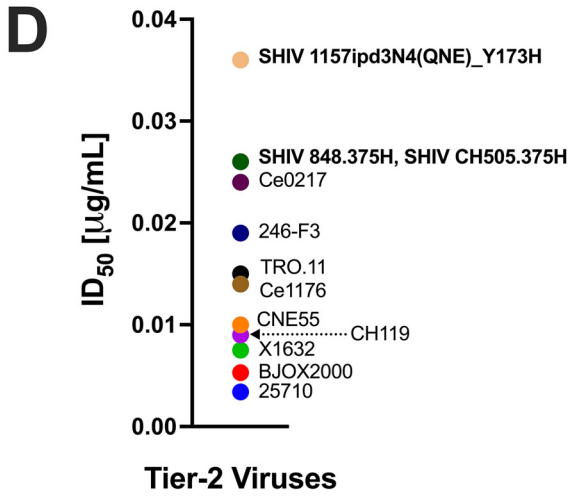

FIG 7 The neutralization potencies of D5_AR IgG against tier-2 HIV-1 viruses are substantially higher in TZM-bl cells expressing FcγRI. (A) Neutralization curves demonstrating the enhanced potency of D5_AR IgG against lentivirus pseudotyped with HIV-1 HXB2 (tier-1B) and 25710 (tier-2) in TZM-bl cells expressing FcγRI versus TZM-bl cells without FcγRI. Data points and error bars are means and standard errors of the means ($n = 2$), respectively. The neutralization curves presented in TZM-bl/FcγRI cells plateaued at around 90% neutralization compared to the 100% neutralization reported in TZM-bl cells; this is possibly explained by varying levels of FcγRI expression on the TZM-bl/FcγRI cells. (B) ID_{50} values and fold enhancement of neutralization potency of D5_AR IgG against lentivirus pseudotyped with HIV-1 HXB2 (tier-1B) and 25710 (tier-2) in TZM-bl cells versus that in TZM-bl/FcγRI cells. D5_AR is potentiated approximately 1,000-fold in TZM-bl/FcγRI cells. (C) ID_{50} values for D5_AR against a panel of tier-2 HIV-1 viruses in TZM-bl/FcγRI cells. Many of the viruses had ID_{50} values below the limit of detection (0.023 μg/ml). (D) ID_{50} values for D5_AR against another panel of tier-2 and SHIV challenge viruses in TZM-bl/FcγRI cells but with a lower limit of detection.

exhibit potentiation (Fig. 8A). This observed potentiation was specific to FcγRI: enhanced neutralization of D5_AR IgG was minimal or not observed in cell lines expressing other Fc receptors (FcγRIIa, FcγRIIb, and FcγRIIIa) (Fig. 8B). It is noteworthy that the ID_{50} values of D5_AR IgG in TZM-bl cells were approximately linearly related to the ID_{50} values in TZM-bl/FcγRI cells (Fig. 9).

DISCUSSION

The PHI of HIV-1 is a validated drug target in humans (50–52), and antibodies that bind the NHR of gp41 that is exposed in the PHI can inhibit HIV-1 infection *in vitro* (53–56, 67). The first of these NHR-binding antibodies, D5, has weak neutralization potency against tier-1 HIV-1 strains (53). We hypothesized that combining multiple CDR mutations from enhanced D5 variants previously described (67) would create a more-effective neutralizing mAb against HIV-1. To test this hypothesis, we evaluated a panel of 16 variants: wild-type D5, four previously described CDR variants (67), and 11 recombined CDR variants (Fig. 2). Here we engineered and characterized a more potent D5 derivative, D5_AR. Using 10 global HIV-1 reference strains, we determined that at modest concentrations, D5_AR neutralizes the majority of tier-1 and tier-2 HIV-1 strains

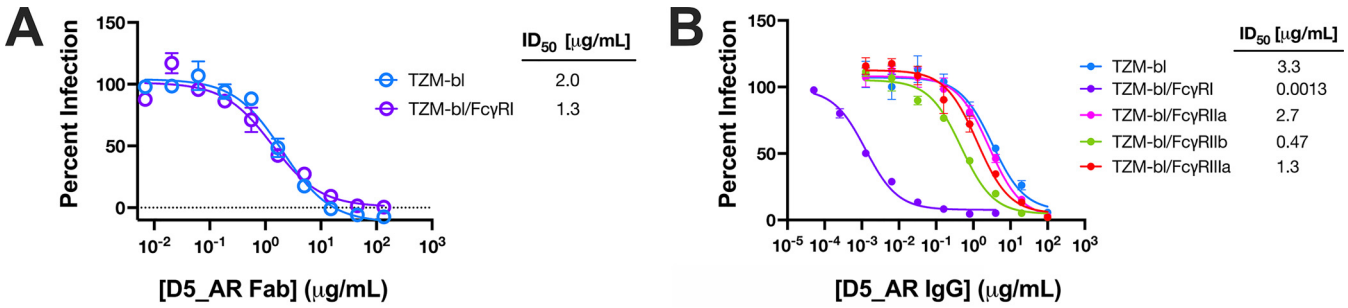

FIG 8 D5_AR is not potentiated as a Fab and shows minimal or no potentiation in the presence of other Fc receptors. (A) Neutralization curves for D5_AR Fab against lentivirus pseudotyped with HIV-1 HXB2 show no neutralization enhancement between TZM-bl cells and TZM-bl/FcγRI cells. Data points and error bars are the means and standard errors of the means ($n = 2$), respectively. (B) The degree of observed neutralization enhancement is FcγRI specific, as demonstrated by the neutralization potency of D5_AR IgG against lentivirus pseudotyped with HIV-1 HXB2 in TZM-bl cells expressing various Fc receptors. Data points and error bars are the means and standard errors of the means ($n = 3$), respectively.

tested from a variety of clades (Fig. 6). Like other anti-NHR antibodies (Fig. 1), D5_AR demonstrates a lower level of somatic hypermutation than bNAbs, with 7.6% of amino acids mutated from germline across both heavy- and light-chain V genes. Taken together with the high sequence conservation of the NHR (https://www.hiv.lanl.gov/content/sequence/HIV/mainpage.html), these proof-of-concept results suggest the PHI, and more specifically, the NHR, is a viable vaccine target.

Several previous reports had suggested that access to the D5 epitope was impacted by steric hindrance, as smaller antibody constructs were more potent than full-length IgG (55, 59, 67, 80). We reinvestigated this issue using antibody preparations that were free of observed protein aggregates (Fig. 5A). In contrast to earlier reports (59, 67, 80), here we confirm (53) that D5 and D5_AR are similarly potent when tested in neutralization assays in scFv, Fab, and IgG formats (Fig. 5). We hypothesize that the presence of higher-order protein aggregates (that can be removed by SEC) may explain the previous reports of size-dependent neutralization by D5. Given these findings for D5 and D5_AR, we conclude that steric hindrance is not an obstacle for at least some anti-PHI antibodies.

Previous work on antibodies targeting another epitope of gp41, the MPER, found that neutralization activity was potentiated as much as 5,000-fold in cells expressing FcγRI, an integral membrane protein that interacts with the Fc portion of γ immunoglobulins (72, 73, 100). Since the MPER is not fully exposed until after Env engages with cellular receptors (101, 102), these results suggest that by binding the Fc region of MPER mAbs, FcγRI provides a local concentration advantage at the cell surface that enhances neutralization (72, 73). Because the PHI, like the MPER, is fully exposed only during the viral membrane fusion

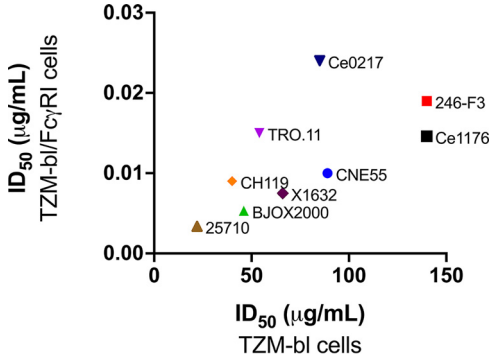

FIG 9 Comparison of HIV-1-neutralizing activity of D5_AR IgG in TZM-bl versus TZM-bl/FcγRI cells. The ID_{50} values of D5_AR IgG in TZM-bl and TZM-bl/FcγRI cells are approximately linearly related in a panel of tier-2 HIV-1 viruses from multiple clades. ID_{50} values represented in this figure were reported previously in Fig. 6 and 7 and selected because they are the only viral isolates for which we conducted neutralization analyses in both TZM-bl and TZM-bl/FcγRI cells.

process, we previously investigated the effect of FcγRI on D5 and found neutralization by this anti-PHI mAb is also enhanced ~5,000-fold (71). Like D5, D5_AR IgG displayed ~1,000-fold enhancement in neutralization potency in TZM-bl/FcγRI cells (Fig. 7A and B). In particular, we have previously demonstrated that D5 potency against HIV-1 HXB2 is enhanced ~6,400-fold in the presence of FcγRI (71) compared to a range of ~1,500-fold (Fig. 7B) to 2,500-fold (Fig. 8B) enhancement for D5_AR against HIV-1 HXB2. We conclude that the enhancement in FcγRI-expressing cells is independent of the effect of the mutations introduced in D5_AR. The magnitude of the potentiation observed by D5_AR is in line with what was previously reported for MPER antibodies and is thus much greater than antibodies to the CD4bs, V2 or V3 loop, or gp41 cluster, which show little to negligible enhancement in cells expressing FcγRI (72, 73). Notably, this enhancement makes D5_AR IgG an extremely potent neutralizing antibody of tier-2 HIV-1 viruses in the TZM-bl/FcγRI cell line, with ID_{50} values of <0.1 μg/ml (Fig. 7C and D).

TZM-bl/FcγRI cells enable sensitive detection of neutralization activity from anti-NHR antibodies and could be used, in conjunction with TZM-bl cells, to monitor progress toward eliciting neutralizing antisera that target the PHI. We hypothesize that neutralizing activity detected by TZM-bl/FcγRI cells could be used as an indicator of low-affinity antibody precursors in serum that have the potential to mature to high-affinity neutralizing activity independent of FcγRI. This hypothesis is supported by our findings that the neutralizing activity of D5_AR in FcγRI-expressing cells was approximately linearly related to the neutralizing activity of D5_AR in cells without FcγRI (Fig. 9).

Although not expressed on $CD4^+$ T cells, FcγRI is expressed on macrophages and dendritic cells (100), which can be productively infected by HIV-1 (103–106), and can then mediate viral transmission to $CD4^+$ T cells (107–110). Importantly, studies of intravaginal inoculation of simian immunodeficiency virus (SIV) of nonhuman primates demonstrated that intraepithelial and submucosal dendritic cells are infected in the earliest stages (18 to 48 h) of SIV infection (111–114). More recent work has shown that at 48 h postinoculation, 25% of infected cells are dendritic cells and macrophages, with the remainder comprising $CD4^+$ T cells, primarily of the Th17 type (115, 116). Thus, it is plausible that inhibiting HIV-1 infection of these FcγRI-expressing cells at the mucosal surfaces by antibodies against the PHI could decrease the likelihood of sexual HIV-1 transmission (71). Indeed, in a vaginal challenge with SHIV in rhesus macaques, an MPER mAb (2F5) afforded dose-dependent protection when administered as an IgG but not when administered in its Fab form (117), suggesting an Fc-dependent mechanism of protection *in vivo*. Previous studies have also demonstrated that MPER mAbs are much more protective against SHIV challenge than other bNAbs when measured *in vitro* (118–121).

While D5_AR does not have the same breadth or potency as bNAbs, D5_AR demonstrates cross-clade tier-2 HIV-1-neutralizing activity and extremely potent activity when measured in cells expressing FcγRI (Fig. 7). These results motivate future efforts to investigate the ability of passively transferred anti-PHI antibodies such as D5_AR to protect against HIV-1 transmission in nonhuman primates. Importantly, D5_AR presents proof of concept that an anti-PHI MAb can neutralize tier-2 HIV-1 viruses. These results will encourage novel vaccine designs against the PHI as an alternative and orthogonal approach for HIV-1 vaccines that is fundamentally different from the prevalent approaches in the field of bNAb and germline-targeting strategies.

MATERIALS AND METHODS

Mammalian expression of D5 constructs. The variable heavy (VH)-chain regions of the D5 variants were ordered as gene fragments from Twist Biosciences. Gene fragments were resuspended to 10 ng/μl in H_2O and PCR amplified using the following two primers: (HC_forward) 5′-ACCGGTGTACATTCCCA GGTTCAAC-3′ and (HC_reverse) 5′-GCCCTTGGTCGACGCGCTTGATACG-3′. The mutated variable light (VL)-chain region, with only the third CDR mutated according to Montgomery et al. (67), was ordered as a gBlock gene fragment from Integrated DNA Technologies and PCR amplified using the following two primers: (LC_forward) 5′-ACCGGTGTACATTCAGATATTCAAATGAC-3′ and (LC_reverse) 5′-TGCAGCCACC GTACGTTTG-3′. Purified VH and VL fragments were cloned into linearized pCMVR with either the human IgG heavy- or kappa light-constant regions, respectively (9, 122). The primers for linearizing the pCMVR

IgG heavy-chain plasmid were (HC_lin_forward) 5′-GCGTCGACCAAGGGCCCATCGGTCTTC-3′ and (HC_lin_reverse) 5′-GGAATGTACACCGGTTGCAGTTGCTACTAGAAAAAG-3′. The primers for linearizing the pCMVR IgG kappa light-chain plasmid were (LC_lin_forward) 5′-CGTACGGTGGCTGCACCATCTGTCTTCATCTTC-3′ and (LC_lin_reverse) 5′-TGAATGTACACCGGTTGCAGTTGCTACTAGAAAAAGGATGATA-3′. The D5 VH and VL segments were cloned into the linearized pCMVR backbones with 5× In-Fusion HD enzyme premix (Takara Bio). Plasmids were transformed into Stellar competent cells (Takara Bio), and transformed cells were grown at 37°C. Colonies were sequence confirmed and then maxiprepped (NucleoBond Xtra Maxi; Macherey-Nagel). Plasmids were sterile filtered using a 0.22-μm syringe filter and stored at −20°C.

D5 IgG variants used for neutralization assays were expressed in Expi293F cells (Thermo Fisher Scientific) using FectoPRO (Polyplus). VH and VL plasmids were cotransfected at a 1:2 ratio, respectively; cells were transfected at 3×10^6 cells/ml. Cell cultures were incubated at 37°C and 8% CO_2 with shaking at 120 rpm. Cells were harvested 3 days posttransfection by spinning at $300 \times g$ for 5 min and then filtered through a 0.22-μm filter. IgG supernatants were diluted 1:1 with 1× phosphate-buffered saline (PBS) and batch bound to Pierce protein A agarose (Thermo Fisher Scientific) overnight at 4°C. The supernatant-resin slurry was added to a column, and the resin was washed with 1× PBS and eluted with 100 mM glycine (pH 2.8) into one-tenth volume of 1 M Tris (pH 8.0).

D5 and D5_AR Fab used for neutralization assays were also produced in Expi293F cells. D5 and D5_AR Fab VH regions were cloned into a pCMVR heavy-chain linearized backbone with a portion (CH2 and CH3 domains) of the constant region removed. Fab VH and VL plasmids were cotransfected and harvested with the protocol for IgG described above. Fab supernatants were diluted 1:1 with 50 mM sodium acetate (pH 5.0), batch bound to Pierce protein G agarose (Thermo Fisher Scientific) overnight at 4°C, washed with 50 mM sodium acetate (pH 5.0), and eluted with 100 mM glycine (pH 2.8) into one-tenth volume of 1 M Tris (pH 8.0).

The complete sequence of the variable heavy region (IGHV1-69 germline) for D5_AR IgG and Fab is QVQLVQSGAEVRKPGASVKVSCKASGDTFSSYAISWVRQAPGQGLEWMGSIIPLFGTAAYAQKFQGRVTITADESTSTAYMELSSLRSEDTAIYYCARDNPTFGAADSWGKGTLVTVSS. The complete sequence of the variable light-chain region (IGKV1-5 germline) for D5_AR IgG and Fab is DIQMTQSPSTLSASIGDRVTITCRASEGIYHWLAWYQQKPGKAPKLLIYKASSLASGAPSRFSGSGSGTDFTLTISSLQPDDFATYYCQQYSNYPLTFGGGTKLEIK.

D5 and D5_AR scFv constructs used for neutralization assays were expressed in Expi293F cells. The VH and VL regions were linked via a linker composed of 20 amino acids (ASTKGPSVKLEEGEFSEARV), tagged with a His_6 tag, and cloned into a linearized pCMVR vector. The scFv plasmid was transfected and harvested with the same protocol as for IgG and Fab. scFv supernatants were diluted 1:1 with 10 mM imidazole in 1× PBS, batch bound to Ni-nitrilotriacetic acid (NTA) agarose (Thermo Fisher Scientific) overnight at 4°C, washed with 10 mM imidazole in 1× PBS, and eluted with 250 mM imidazole in 1× PBS.

The complete sequence of the D5_AR scFv insert is QVQLVQSGAEVRKPGASVKVSCKASGDTFSSYAISWVRQAPGQGLEWMGSIIPLFGTAAYAQKFQGRVTITADESTSTAYMELSSLRSEDTAIYYCARDNPTFGAADSWGKGTLVTVSSASTKGPSVKLEEGEFSEARVDIQMTQSPSTLSASIGDRVTITCRASEGIYHWLAWYQQKPGKAPKLLIYKASSLASGAPSRFSGSGSGTDFTLTISSLQPDDFATYYCQQYSNYPLTFGGGTKLEIKAAALEHHHHHH.

Purification and storage of D5 constructs. For the initial screening in neutralization assays (Table 1), there was no purification following elution from protein A affinity purification. Elutions were buffer exchanged and spin concentrated using 1× PBS and Amicon Ultra-15 10-kDa 15-ml spin concentrators (Millipore).

For all other neutralization assays, elutions were further purified after affinity purification on an AKTA using a GE Superdex 200 Increase 10/300 GL column (GE HealthCare) in 1× PBS. After size exclusion chromatography, samples were spin concentrated using Amicon Ultra-15 10-kDa 15-ml spin concentrators.

Fab and scFv constructs were eluted from affinity purification and then purified further via size exclusion chromatography using the Superdex 200 Increase 10/300 GL column (GE HealthCare) and 1× PBS. Samples were spin concentrated as described above.

For all samples, regardless of the purification procedure, concentrated elution samples were syringe filtered using a 0.22-μm filter and stored at 4°C prior to use.

Synthesis of covalent biotinylated CCIZN17. Biotinylated CCIZN17 (CCGGIKKEIEAIKKEQEAIKKKIEAIEKLLQLTVWGIKQLQARIL) was synthesized using standard Fmoc-based solid-phase peptide synthesis on a CSBio instrument. The resin was 250 μmol NovaSyn TGR R resin (Novabiochem), and coupling was performed for 15 min at 60°C with 4-fold molar excess of amino acids. Biotin was installed on the N terminus via coupling with biotin-polyethylene glycol $(PEG)_4$-propionic acid (ChemPep). Dry peptide resin was cleaved with 94% trifluoroacetic acid, 2.5% water, 2.5% 1,2-ethanediol, and 1% triisopropylsilane at room temperature for 3.5 h followed by precipitation in cold diethyl ether. The crude peptide was purified by reversed-phase high-pressure liquid chromatography (HPLC) on a C_{18} semiprep column over an acetonitrile (ACN) gradient in the presence of 0.1% trifluoroacetic acid (TFA), and fractions were collected based on liquid chromatography-mass spectrometry (LC/MS) analysis. The pure monomeric protein was dissolved to 1 mg/ml in 100 mM Tris-HCl (pH 8.0) and oxidized by air at 37°C with gentle shaking for 48 h. The peptide mixture was then lyophilized, dissolved into 20% ACN-80% water, and repurified via HPLC. Peptide product whose mass corresponded to that of three biotinylated-CCIZN17 peptide chains linked by three-disulfide bridges was collected.

Biolayer interferometry. Biotinylated CCIZN17 peptide (200 nM) was loaded on streptavidin biosensors (Pall ForteBio) to a load threshold of 0.4 nm using an Octet RED96 system (Pall ForteBio). Sensors were immediately regenerated in 100 mM glycine (pH 1.5) and neutralized to remove aggregates and nonspecific interactions. Ligand-loaded sensors were dipped into known concentrations of Fab for an association step (4 min) and returned to the baseline well for a dissociation step (4 min). All reactions

were run in PBS (pH 7.4) with 0.1% bovine serum albumin (BSA) and 0.05% Tween 20. All samples in all experiments were baseline subtracted to a well that loaded the tip with biotinylated peptide but did not go into the sample as a control for any buffer trends within the samples. Association/dissociation binding curves were fit in GraphPad Prism 8 using the "Association then Dissociation" analysis to calculate the equilibrium dissociation constant (K_D), k_{on}, and k_{off}. Averages from fitted values across multiple concentrations from at least two independent experiments are reported.

Transfection to produce HIV-1 pseudotyped lentiviruses. HEK293T cells were transiently cotransfected with a backbone plasmid as well as an HIV-1 Env plasmid for HIV-1 pseudotyped lentivirus production using the calcium phosphate transfection protocol previously described (123–125). HEK293T cells were passaged in T75 flasks and incubated at 37°C at 5% CO_2. The growth medium used for passaging and transfections was Corning Dulbecco's modified eagle medium (DMEM; with 4.5 g/liter glucose, L-glutamine, and sodium pyruvate) with 10% fetal bovine serum, 1% penicillin-streptomycin (Corning), and 1% L-glutamine (Corning).

The backbone plasmid psg3ΔEnv was obtained through the NIH AIDS Reagent Program, Division of AIDS, NIAID, NIH from John C. Kappes and Xiaoyun Wu: HIV-1 SG3 ΔEnv noninfectious molecular clone (catalog number 11051) (126, 127). The psg3ΔEnv plasmid was propagated in MAX Efficiency Stbl2 cells grown at 30°C with shaking, and Env plasmids were propagated in Stellar competent cells grown at 37°C with shaking. DNA was isolated using a maxiprep kit (NucleoBond Xtra Maxi; Macherey-Nagel) and sequence confirmed.

In brief, 6×10^6 HEK293T cells were plated in 10-cm petri dishes in a total volume of 10 ml of DMEM and incubated overnight at 37°C and 5% CO_2 without shaking. Once the cells reached 50% to 80% confluence, they were transfected as follows. In a Falcon tube, 20 μg of psg3ΔEnv was mixed with 10 μg of Env plasmid and water for a final volume of 500 μl. Five hundred microliters of 2× HEPES-buffered saline (pH 7) (Alfa Aesar) was added dropwise to the mixture, and 100 μl 2.5 M $CaCl_2$ was added subsequently. The mixture was incubated at room temperature for 20 min and then added dropwise onto the cells. Next, 12 to 18 h after transfection, the medium was aspirated from the dish and replaced with 10 ml of fresh DMEM with additives. Virus-containing medium was harvested 48 h after the medium swap and centrifuged at 300 × *g* for 5 min; the supernatant was sterile filtered with a 0.45-μm polyvinylidene difluoride filter and stored in 1-ml aliquots at −80°C.

Neutralization assay. The neutralization assay was adapted from the TZM-bl assay protocol using HIV-1 Env-pseudotyped viruses as described previously (75, 78). Briefly, TZM-bl cells, derived from the JC53-bl parental cell line, were used as reporter cells in this assay and were obtained through the NIH AIDS Reagent Program (catalog number 8129) from John C. Kappes and Xiaoyun Wu (126, 128–131). TZM-bl cells are adherent HeLa cells that stably express CD4 and CCR5 and constitutively express CXCR4; they have integrated β-galactosidase and firefly luciferase reporter genes under the control of the HIV-1 long terminal repeat (LTR) promoter. TZM-bl cells transduced to stably express FcγRI (72, 73) were also used in these neutralization assays. TZM-bl cells were passaged in T25 flasks and incubated at 37°C at 5% CO_2 without shaking. The growth medium used for passaging and neutralization assays was Corning DMEM with 10% fetal bovine serum, 1% penicillin-streptomycin (Corning), and 1% L-glutamine (Corning).

In brief, 5×10^3 TZM-bl cells were plated in the internal 60 wells of white-walled, clear-bottom 96-well plates and incubated overnight at 37°C at 5% CO_2 without shaking. All outside wells were filled with 200 μl PBS to minimize evaporation. On the next day, the medium was aspirated without disturbing the cells and replaced with a final mixture composed of one-half volume DMEM, one-fourth volume HIV-1 pseudotyped lentivirus, one-fourth volume D5 antibody at varying concentrations, and DEAE dextran (10 μg/ml). Forty-eight hours after infection, all medium was aspirated off the wells, cells were lysed, and either luciferase activity was determined using BriteLite Plus reagent (Perkin Elmer) or β-galactosidase activity was determined using Tropix Gal-Screen (Applied Biosystems) and buffer A (Applied Biosystems). β-Galactosidase readout was used for neutralizations show in Table 1 and Fig. 4, 5, and 6. Luciferase readout was used for neutralizations shown in Fig. 7 and 8.

Relative luminescence unit (RLU) values were quantified using a Synergy HTX multimode reader (BioTek), normalized against cells-only reference wells, and averaged for technical replicates on the plate. Percent infectivity and propagated error values (see "Statistics and data analysis") were entered into GraphPad Prism 8. Neutralization titers are reported as the antibody concentration at which RLUs were reduced by 50% compared to RLUs in virus control wells after subtraction of background RLU in cell control wells. ID_{50} was calculated using the inhibitor concentration versus response (three parameters) dose-response curve fit in GraphPad Prism 8. This assay was conducted in compliance with good clinical laboratory procedures (GCLP) (132), including participation in a formal TZM-bl assay proficiency program for GCLP-compliant laboratories (74).

Statistics and data analysis. Percent infectivity for the neutralization assays was calculated as follows:

$$\left(\frac{\text{sample RLU} - \text{cells} - \text{only RLU}}{\text{virus} - \text{only RLU} - \text{cells} - \text{only RLU}}\right) \times 100.$$

Propagated error for the percent infectivity was calculated using the following formula:

$$(\%\text{infection}) \times \sqrt{\left(\frac{\text{STD of sample RLU}}{\text{AVG of sample RLU}}\right)^2 + \left(\frac{\text{STD of virus} - \text{only RLU}}{\text{AVG of virus} - \text{only RLU}}\right)^2},$$

where STD is the standard deviation and AVG is the average. The ID_{50} values in Table 1 and Fig. 6 represent the geometric means from the biological replicates for the tested antibodies with the standard

errors of the means reported. Fold difference in ID_{50} was calculated for each experiment by dividing the D5 ID_{50} by the D5 variant ID_{50}. Because fold difference was calculated for each experiment, the reported fold differences in Table 1 are the geometric means and the standard errors of the means from all replicates.

ACKNOWLEDGMENTS

We thank members of the Kim Lab for helpful discussions and A. E. Powell, S. Tang, and D. Xu for critical readings of this manuscript.

This research was supported by the National Institutes of Health under award numbers T32GM007276 (B.N.B.), T32GM007365 (M.V.F.I.), and DP1DA043893 (P.S.K.), the NSF GRFP (B.N.B.), NIH/NIAID contract HHSN272201800004C (C.C.L.), Bill and Melinda Gates Foundation award OPP1113682 (P.S.K.), the Virginia and D. K. Ludwig Fund for Cancer Research (P.S.K.), and the Chan Zuckerberg Biohub (P.S.K.).

A.A.R., M.V.F.I., C.L.B., and P.S.K. conceived the experiments. A.A.R. performed protein purification, antibody characterization, and neutralization assays. M.V.F.I. and B.N.B. performed protein purification and neutralization assays. T.U.J.B. performed protein purification. Additional neutralization assays were also conducted under the supervision of C.C.L. and D.C.M. All authors contributed to revising the manuscript.

REFERENCES

1. Rerks-Ngarm S, Pitisuttithum P, Nitayaphan S, Kaewkungwal J, Chiu J, Paris R, Premsri N, Namwat C, de Souza M, Adams E, Benenson M, Gurunathan S, Tartaglia J, McNeil JG, Francis DP, Stablein D, Birx DL, Chunsuttiwat S, Khamboonruang C, Thongcharoen P, Robb ML, Michael NL, Kunasol P, Kim JH, MOPH-TAVEG Investigators. 2009. Vaccination with ALVAC and AIDSVAX to prevent HIV-1 infection in Thailand. N Engl J Med 361:2209–2220. https://doi.org/10.1056/NEJMoa0908492.
2. Adepoju P. 2020. Moving on from the failed HIV vaccine clinical trial. Lancet HIV 7:e161. https://doi.org/10.1016/S2352-3018(20)30047-3.
3. Burton DR, Pyati J, Koduri R, Sharp SJ, Thornton GB, Parren PWHI, Sawyer LSW, Hendry RM, Dunlop N, Nara PL, Lamacchia M, Garratty E, Stiehm ER, Bryson YJ, Cao Y, Moore JP, Ho DD, Barbas CF. 1994. Efficient neutralization of primary isolates of HIV-1 by a recombinant human monoclonal antibody. Science 266:1024–1027. https://doi.org/10.1126/science.7973652.
4. Scheid JF, Mouquet H, Feldhahn N, Seaman MS, Velinzon K, Pietzsch J, Ott RG, Anthony RM, Zebroski H, Hurley A, Phogat A, Chakrabarti B, Li Y, Connors M, Pereyra F, Walker BD, Wardemann H, Ho D, Wyatt RT, Mascola JR, Ravetch JV, Nussenzweig MC. 2009. Broad diversity of neutralizing antibodies isolated from memory B cells in HIV-infected individuals. Nature 458:636–640. https://doi.org/10.1038/nature07930.
5. Kwong PD, Mascola JR. 2018. HIV-1 vaccines based on antibody identification, B cell ontogeny, and epitope structure. Immunity 48:855–871. https://doi.org/10.1016/j.immuni.2018.04.029.
6. Bricault CA, Yusim K, Seaman MS, Yoon H, Theiler J, Giorgi EE, Wagh K, Theiler M, Hraber P, Macke JP, Kreider EF, Learn GH, Hahn BH, Scheid JF, Kovacs JM, Shields JL, Lavine CL, Ghantous F, Rist M, Bayne MG, Neubauer GH, McMahan K, Peng H, Chéneau C, Jones JJ, Zeng J, Ochsenbauer C, Nkolola JP, Stephenson KE, Chen B, Gnanakaran S, Bonsignori M, Williams LTD, Haynes BF, Doria-Rose N, Mascola JR, Montefiori DC, Barouch DH, Korber B. 2019. HIV-1 neutralizing antibody signatures and application to epitope-targeted vaccine design. Cell Host Microbe 25:59–72. https://doi.org/10.1016/j.chom.2018.12.001.
7. Xiao X, Chen W, Feng Y, Zhu Z, Prabakaran P, Wang Y, Zhang MY, Longo NS, Dimitrov DS. 2009. Germline-like predecessors of broadly neutralizing antibodies lack measurable binding to HIV-1 envelope glycoproteins: implications for evasion of immune responses and design of vaccine immunogens. Biochem Biophys Res Commun 390:404–409. https://doi.org/10.1016/j.bbrc.2009.09.029.
8. Zhou T, Georgiev I, Wu X, Yang ZY, Dai K, Finzi A, Kwon Y, Scheid JF, Shi W, Xu L, Yang Y, Zhu J, Nussenzweig MC, Sodroski J, Shapiro L, Nabel GJ, Mascola JR, Kwong PD. 2010. Structural basis for broad and potent neutralization of HIV-1 by antibody VRC01. Science 329:811–817. https://doi.org/10.1126/science.1192819.
9. Wu X, Yang Z-Y, Li Y, Hogerkorp C-M, Schief WR, Seaman MS, Zhou T, Schmidt SD, Wu L, Xu L, Longo NS, McKee K, O'Dell S, Louder MK, Wycuff DL, Feng Y, Nason M, Doria-Rose N, Connors M, Kwong PD, Roederer M, Wyatt RT, Nabel GJ, Mascola JR. 2010. Rational design of envelope identifies broadly neutralizing human monoclonal antibodies to HIV-1. Science 329:856–861. https://doi.org/10.1126/science.1187659.
10. Jardine J, Julien JP, Menis S, Ota T, Kalyuzhniy O, McGuire A, Sok D, Huang PS, MacPherson S, Jones M, Nieusma T, Mathison J, Baker D, Ward AB, Burton DR, Stamatatos L, Nemazee D, Wilson IA, Schief WR. 2013. Rational HIV immunogen design to target specific germline B cell receptors. Science 340:711–716. https://doi.org/10.1126/science.1234150.
11. Liao HX, Lynch R, Zhou T, Gao F, Munir Alam S, Boyd SD, Fire AZ, Roskin KM, Schramm CA, Zhang Z, Zhu J, Shapiro L, NISC Comparative Sequencing Program, Mullikin JC, Gnanakaran S, Hraber P, Wiehe K, Kelsoe G, Yang G, Xia S-M, Montefiori DC, Parks R, Lloyd KE, Scearce RM, Soderberg KA, Cohen M, Kamanga G, Louder MK, Tran LM, Chen Y, Cai F, Chen S, Moquin S, Du X, Joyce MG, Srivatsan S, Zhang B, Zheng A, Shaw GM, Hahn BH, Kepler TB, Korber BTM, Kwong PD, Mascola JR, Haynes BF. 2013. Co-evolution of a broadly neutralizing HIV-1 antibody and founder virus. Nature 496:469–476. https://doi.org/10.1038/nature12053.
12. McGuire AT, Hoot S, Dreyer AM, Lippy A, Stuart A, Cohen KW, Jardine J, Menis S, Scheid JF, West AP, Schief WR, Stamatatos L. 2013. Engineering HIV envelope protein to activate germline B cell receptors of broadly neutralizing anti-CD4 binding site antibodies. J Exp Med 210:655–663. https://doi.org/10.1084/jem.20122824.
13. Sather DN, Carbonetti S, Malherbe DC, Pissani F, Stuart AB, Hessell AJ, Gray MD, Mikell I, Kalams SA, Haigwood NL, Stamatatos L. 2014. Emergence of broadly neutralizing antibodies and viral coevolution in two subjects during the early stages of infection with human immunodeficiency virus type 1. J Virol 88:12968–12981. https://doi.org/10.1128/JVI.01816-14.
14. Huang J, Kang BH, Ishida E, Zhou T, Griesman T, Sheng Z, Wu F, Doria-Rose NA, Zhang B, McKee K, O'Dell S, Chuang G-Y, Druz A, Georgiev IS, Schramm CA, Zheng A, Joyce MG, Asokan M, Ransier A, Darko S, Migueles SA, Bailer RT, Louder MK, Alam SM, Parks R, Kelsoe G, Von Holle T, Haynes BF, Douek DC, Hirsch V, Seaman MS, Shapiro L, Mascola JR, Kwong PD, Connors M. 2016. Identification of a CD4-binding-site antibody to HIV that evolved near-pan neutralization breadth. Immunity 45:1108–1121. https://doi.org/10.1016/j.immuni.2016.10.027.
15. Jardine JG, Kulp DW, Havenar-Daughton C, Sarkar A, Briney B, Sok D, Sesterhenn F, Ereno-Orbea J, Kalyuzhniy O, Deresa I, Hu X, Spencer S, Jones M, Georgeson E, Adachi Y, Kubitz M, DeCamp AC, Julien J-P, Wilson IA, Burton DR, Crotty S, Schief WR. 2016. HIV-1 broadly neutralizing antibody precursor B cells revealed by germline-targeting immunogen. Science 351:1458–1463. https://doi.org/10.1126/science.aad9195.
16. McGuire AT, Gray MD, Dosenovic P, Gitlin AD, Freund NT, Petersen J, Correnti C, Johnsen W, Kegel R, Stuart AB, Glenn J, Seaman MS, Schief WR, Strong RK, Nussenzweig MC, Stamatatos L. 2016. Specifically modified Env immunogens activate B-cell precursors of broadly neutralizing HIV-1 antibodies in transgenic mice. Nat Commun 7:10618. https://doi.org/10.1038/ncomms10618.

17. Bonsignori M, Kreider EF, Fera D, Meyerhoff RR, Bradley T, Wiehe K, Alam SM, Aussedat B, Walkowicz WE, Hwang KK, Saunders KO, Zhang R, Gladden MA, Monroe A, Kumar A, Xia SM, Cooper M, Louder MK, McKee K, Bailer RT, Pier BW, Jette CA, Kelsoe G, Williams WB, Morris L, Kappes J, Wagh K, Kamanga G, Cohen MS, Hraber PT, Montefiori DC, Trama A, Liao HX, Kepler TB, Moody MA, Gao F, Danishefsky SJ, Mascola JR, Shaw GM, Hahn BH, Harrison SC, Korber BT, Haynes BF. 2017. Staged induction of HIV-1 glycan-dependent broadly neutralizing antibodies. Sci Transl Med 9:eaai7514. https://doi.org/10.1126/scitranslmed.aai7514.
18. Escolano A, Dosenovic P, Nussenzweig MC. 2017. Progress toward active or passive HIV-1 vaccination. J Exp Med 214:3–16. https://doi.org/10.1084/jem.20161765.
19. Haynes BF, Burton DR. 2017. Developing an HIV vaccine. Science 355:1129–1130. https://doi.org/10.1126/science.aan0662.
20. Verkoczy L. 2017. Humanized immunoglobulin mice: models for HIV vaccine testing and studying the broadly neutralizing antibody problem, p 235–352. *In* Advances in Immunology, 1st ed. Elsevier Inc., Amsterdam, Netherlands.
21. Havenar-Daughton C, Abbott RK, Schief WR, Crotty S. 2018. When designing vaccines, consider the starting material: the human B cell repertoire. Curr Opin Immunol 53:209–216. https://doi.org/10.1016/j.coi.2018.08.002.
22. Havenar-Daughton C, Sarkar A, Kulp DW, Toy L, Hu X, Deresa I, Kalyuzhniy O, Kaushik K, Upadhyay AA, Menis S, Landais E, Cao L, Diedrich JK, Kumar S, Schiffner T, Reiss SM, Seumois G, Yates JR, Paulson JC, Bosinger SE, Wilson IA, Schief WR, Crotty S. 2018. The human naive B cell repertoire contains distinct subclasses for a germline-targeting HIV-1 vaccine immunogen. Sci Transl Med 10:eaat0381. https://doi.org/10.1126/scitranslmed.aat0381.
23. Wibmer CK, Moore PL, Morris L. 2015. HIV broadly neutralizing antibody targets. Curr Opin HIV AIDS 10:135–143. https://doi.org/10.1097/COH.0000000000000153.
24. McCoy LE. 2018. The expanding array of HIV broadly neutralizing antibodies. Retrovirology 15:70. https://doi.org/10.1186/s12977-018-0453-y.
25. Mascola JR, Haynes BF. 2013. HIV-1 neutralizing antibodies: understanding nature's pathways. Immunol Rev 254:225–244. https://doi.org/10.1111/imr.12075.
26. Pancera M, Changela A, Kwong PD. 2017. How HIV-1 entry mechanism and broadly neutralizing antibodies guide structure-based vaccine design. Curr Opin HIV AIDS 12:229–240. https://doi.org/10.1097/COH.0000000000000360.
27. McGuire AT, Glenn JA, Lippy A, Stamatatos L. 2014. Diverse recombinant HIV-1 Envs fail to activate B cells expressing the germline B cell receptors of the broadly neutralizing anti-HIV-1 antibodies PG9 and 447-52D. J Virol 88:2645–2657. https://doi.org/10.1128/JVI.03228-13.
28. Hoot S, McGuire AT, Cohen KW, Strong RK, Hangartner L, Klein F, Diskin R, Scheid JF, Sather DN, Burton DR, Stamatatos L. 2013. Recombinant HIV envelope proteins fail to engage germline versions of anti-CD4bs bNAbs. PLoS Pathog 9:e1003106. https://doi.org/10.1371/journal.ppat.1003106.
29. Xu K, Acharya P, Kong R, Cheng C, Chuang G-Y, Liu K, Louder MK, O'Dell S, Rawi R, Sastry M, Shen C-H, Zhang B, Zhou T, Asokan M, Bailer RT, Chambers M, Chen X, Choi CW, Dandey VP, Doria-Rose NA, Druz A, Eng ET, Farney SK, Foulds KE, Geng H, Georgiev IS, Gorman J, Hill KR, Jafari AJ, Kwon YD, Lai Y-T, Lemmin T, McKee K, Ohr TY, Ou L, Peng D, Rowshan AP, Sheng Z, Todd J-P, Tsybovsky Y, Viox EG, Wang Y, Wei H, Yang Y, Zhou AF, Chen R, Yang L, Scorpio DG, McDermott AB, Shapiro L, et al. 2018. Epitope-based vaccine design yields fusion peptide-directed antibodies that neutralize diverse strains of HIV-1. Nat Med 24:857–867. https://doi.org/10.1038/s41591-018-0042-6.
30. Pauthner M, Havenar-Daughton C, Sok D, Nkolola JP, Bastidas R, Boopathy AV, Carnathan DG, Chandrashekar A, Cirelli KM, Cottrell CA, Eroshkin AM, Guenaga J, Kaushik K, Kulp DW, Liu J, McCoy LE, Oom AL, Ozorowski G, Post KW, Sharma SK, Steichen JM, de Taeye SW, Tokatlian T, Torrents de la Peña A, Butera ST, LaBranche CC, Montefiori DC, Silvestri G, Wilson IA, Irvine DJ, Sanders RW, Schief WR, Ward AB, Wyatt RT, Barouch DH, Crotty S, Burton DR. 2017. Elicitation of robust tier 2 neutralizing antibody responses in nonhuman primates by HIV envelope trimer immunization using optimized approaches. Immunity 46:1073–1088. https://doi.org/10.1016/j.immuni.2017.05.007.
31. Saunders KO, Nicely NI, Wiehe K, Bonsignori M, Meyerhoff RR, Parks R, Walkowicz WE, Aussedat B, Wu NR, Cai F, Vohra Y, Park PK, Eaton A, Go EP, Sutherland LL, Scearce RM, Barouch DH, Zhang R, Von Holle T, Overman RG, Anasti K, Sanders RW, Moody MA, Kepler TB, Korber B, Desaire H, Santra S, Letvin NL, Nabel GJ, Montefiori DC, Tomaras GD, Liao HX, Alam SM, Danishefsky SJ, Haynes BF. 2017. Vaccine elicitation of high mannose-dependent neutralizing antibodies against the V3-glycan broadly neutralizing epitope in nonhuman primates. Cell Rep 18:2175–2188. https://doi.org/10.1016/j.celrep.2017.02.003.
32. Chan DC, Kim PS. 1998. HIV entry and its inhibition. Cell 93:681–684. https://doi.org/10.1016/s0092-8674(00)81430-0.
33. Harrison SC. 2015. Viral membrane fusion. Virology 479–480:498–507. https://doi.org/10.1016/j.virol.2015.03.043.
34. Ladinsky MS, Gnanapragasam PN, Yang Z, West AP, Kay MS, Bjorkman PJ. 2020. Electron tomography visualization of HIV-1 fusion with target cells using fusion inhibitors to trap the pre-hairpin intermediate. Elife 9:e58411. https://doi.org/10.7554/eLife.58411.
35. Eckert DM, Malashkevich VN, Hong LH, Carr PA, Kim PS. 1999. Inhibiting HIV-1 entry: discovery of D-peptide inhibitors that target the gp41 coiled-coil pocket. Cell 99:103–115. https://doi.org/10.1016/s0092-8674(00)80066-5.
36. Root MJ, Kay MS, Kim PS. 2001. Protein design of an HIV-1 entry inhibitor. Science 291:884–888. https://doi.org/10.1126/science.1057453.
37. Zhu Y, Su S, Qin L, Wang Q, Shi L, Ma Z, Tang J, Jiang S, Lu L, Ye S, Zhang R. 2016. Rational improvement of gp41-targeting HIV-1 fusion inhibitors: an innovatively designed Ile-Asp-Leu tail with alternative conformations. Sci Rep 6:31983. https://doi.org/10.1038/srep31983.
38. Wang H, Qi Z, Guo A, Mao Q, Lu H, An X, Xia C, Li X, Debnath AK, Wu S, Liu S, Jiang S. 2009. ADS-J1 inhibits human immunodeficiency virus type 1 entry by interacting with the gp41 pocket region and blocking fusion-active gp41 core formation. Antimicrob Agents Chemother 53:4987–4998. https://doi.org/10.1128/AAC.00670-09.
39. Welch BD, Francis JN, Redman JS, Paul S, Weinstock MT, Reeves JD, Lie YS, Whitby FG, Eckert DM, Hill CP, Root MJ, Kay MS. 2010. Design of a potent D-peptide HIV-1 entry inhibitor with a strong barrier to resistance. J Virol 84:11235–11244. https://doi.org/10.1128/JVI.01339-10.
40. Qiu J, Liang T, Wu J, Yu F, He X, Tian Y, Xie L, Jiang S, Liu S, Li L. 2019. N-Substituted pyrrole derivative 12M inhibits HIV-1 entry by targeting gp41 of HIV-1 envelope glycoprotein. Front Pharmacol 10:859. https://doi.org/10.3389/fphar.2019.00859.
41. Liu S, Wu S, Jiang S. 2007. HIV entry inhibitors targeting gp41: from polypeptides to small-molecule compounds. Curr Pharm Des 13:143–162. https://doi.org/10.2174/138161207779313722.
42. Yi HA, Fochtman BC, Rizzo RC, Jacobs A. 2016. Inhibition of HIV entry by targeting the envelope transmembrane subunit gp41. Curr HIV Res 14:283–294. https://doi.org/10.2174/1570162x14999160224103908.
43. Jiang S, Lin K, Strick N, Neurath AR. 1993. HIV-1 inhibition by a peptide. Nature 365:113. https://doi.org/10.1038/365113a0.
44. He Y, Cheng J, Lu H, Li J, Hu J, Qi Z, Liu Z, Jiang S, Dai Q. 2008. Potent HIV fusion inhibitors against Enfuvirtide-resistant HIV-1 strains. Proc Natl Acad Sci U S A 105:16332–16337. https://doi.org/10.1073/pnas.0807335105.
45. Ferrer M, Kapoor TM, Strassmaier T, Weissenhorn W, Skehel JJ, Oprian D, Schreiber SL, Wiley DC, Harrison SC. 1999. Selection of gp41-mediated HIV-1 cell entry inhibitors from biased combinatorial libraries of non-natural binding elements. Nat Struct Biol 6:953–960. https://doi.org/10.1038/13324.
46. Wild C, Dubay JW, Greenwell T, Baird T, Oas TG, Mcdanal C, Hunter E, Matthews T. 1994. Propensity for a leucine zipper-like domain of human immunodeficiency virus type 1 gp41 to form oligomers correlates with a role in virus-induced fusion rather than assembly of the glycoprotein complex. Proc Natl Acad Sci U S A 91:12676–12680. https://doi.org/10.1073/pnas.91.26.12676.
47. Lu M, Blacklow SC, Kim PS. 1995. A trimeric structural domain of the HIV-1 transmembrane glycoprotein. Nat Struct Biol 2:1075–1082. https://doi.org/10.1038/nsb1295-1075.
48. Pan C, Liu S, Jiang S. 2010. HIV-1 gp41 fusion intermediate: a target for HIV therapeutics. J Formos Med Assoc 109:94–105. https://doi.org/10.1016/S0929-6646(10)60029-0.
49. Nishimura Y, Francis JN, Donau OK, Jesteadt E, Sadjadpour R, Smith AR, Seaman MS, Welch BD, Martin MA, Kay MS. 2020. Prevention and treatment of SHIVAD8 infection in rhesus macaques by a potent D-peptide HIV entry inhibitor. Proc Natl Acad Sci U S A 117:22436–22442. https://doi.org/10.1073/pnas.2009700117.
50. Wild C, Greenwell T, Matthews T. 1993. A synthetic peptide from HIV-1 gp41 is a potent inhibitor of virus-mediated cell-cell fusion. AIDS Res Hum Retroviruses 9:1051–1053. https://doi.org/10.1089/aid.1993.9.1051.
51. Kilby JM, Lalezari JP, Eron JJ, Carlson M, Cohen C, Arduino RC, Goodgame JC, Gallant JE, Volberding P, Murphy RL, Valentine F, Saag MS, Nelson EL, Sista PR, Dusek A. 2002. The safety, plasma pharmacokinetics, and antiviral activity of subcutaneous enfuvirtide (T-20), a peptide inhibitor of gp41-mediated

virus fusion, in HIV-infected adults. AIDS Res Hum Retroviruses 18:685–693. https://doi.org/10.1089/088922202760072294.
52. Matthews T, Salgo M, Greenberg M, Chung J, DeMasi R, Bolognesi D. 2004. Enfuvirtide: the first therapy to inhibit the entry of HIV-1 into host CD4 lymphocytes. Nat Rev Drug Discov 3:215–225. https://doi.org/10.1038/nrd1331.
53. Miller MD, Geleziunas R, Bianchi E, Lennard S, Hrin R, Zhang H, Lu M, An Z, Ingallinella P, Finotto M, Mattu M, Finnefrock AC, Bramhill D, Cook J, Eckert DM, Hampton R, Patel M, Jarantow S, Joyce J, Ciliberto G, Cortese R, Lu P, Strohl W, Schleif W, McElhaugh M, Lane S, Lloyd C, Lowe D, Osbourn J, Vaughan T, Emini E, Barbato G, Kim PS, Hazuda DJ, Shiver JW, Pessi A. 2005. A human monoclonal antibody neutralizes diverse HIV-1 isolates by binding a critical gp41 epitope. Proc Natl Acad Sci U S A 102:14759–14764. https://doi.org/10.1073/pnas.0506927102.
54. Gustchina E, Li M, Louis JM, Eric Anderson D, Lloyd J, Frisch C, Bewley CA, Gustchina A, Wlodawer A, Marius Clore G. 2010. Structural basis of HIV-1 neutralization by affinity matured Fabs directed against the internal trimeric coiled-coil of gp41. PLoS Pathog 6:e1001182. https://doi.org/10.1371/journal.ppat.1001182.
55. Sabin C, Corti D, Buzon V, Seaman MS, Hulsik DL, Hinz A, Vanzetta F, Agatic G, Silacci C, Mainetti L, Scarlatti G, Sallusto F, Weiss R, Lanzavecchia A, Weissenhorn W. 2010. Crystal structure and size-dependent neutralization properties of HK20, a human monoclonal antibody binding to the highly conserved heptad repeat 1 of gp41. PLoS Pathog 6:e1001195. https://doi.org/10.1371/journal.ppat.1001195.
56. Nelson JD, Kinkead H, Brunel FM, Leaman D, Jensen R, Louis JM, Maruyama T, Bewley CA, Bowdish K, Clore GM, Dawson PE, Frederickson S, Mage RG, Richman DD, Burton DR, Zwick MB. 2008. Antibody elicited against the gp41 N-heptad repeat (NHR) coiled-coil can neutralize HIV-1 with modest potency but non-neutralizing antibodies also bind to NHR mimetics. Virology 377:170–183. https://doi.org/10.1016/j.virol.2008.04.005.
57. Corti D, Langedijk JPM, Hinz A, Seaman MS, Vanzetta F, Fernandez-Rodriguez BM, Silacci C, Pinna D, Jarrossay D, Balla-Jhagjhoorsingh S, Willems B, Zekveld MJ, Dreja H, O'Sullivan E, Pade C, Orkin C, Jeffs SA, Montefiori DC, Davis D, Weissenhorn W, McKnight A, Heeney JL, Sallusto F, Sattentau QJ, Weiss RA, Lanzavecchia A. 2010. Analysis of memory B cell responses and isolation of novel monoclonal antibodies with neutralizing breadth from HIV-1-infected individuals. PLoS One 5:e8805. https://doi.org/10.1371/journal.pone.0008805.
58. Eckert DM, Kim PS. 2001. Design of potent inhibitors of HIV-1 entry from the gp41 N-peptide region. Proc Natl Acad Sci U S A 98:11187–11192. https://doi.org/10.1073/pnas.201392898.
59. Luftig MA, Mattu M, Di Giovine P, Geleziunas R, Hrin R, Barbato G, Bianchi E, Miller MD, Pessi A, Carfí A. 2006. Structural basis for HIV-1 neutralization by a gp41 fusion intermediate-directed antibody. Nat Struct Mol Biol 13:740–747. https://doi.org/10.1038/nsmb1127.
60. Bonsignori M, Hwang K-K, Chen X, Tsao C-Y, Morris L, Gray E, Marshall DJ, Crump JA, Kapiga SH, Sam NE, Sinangil F, Pancera M, Yongping Y, Zhang B, Zhu J, Kwong PD, O'Dell S, Mascola JR, Wu L, Nabel GJ, Phogat S, Seaman MS, Whitesides JF, Moody MA, Kelsoe G, Yang X, Sodroski J, Shaw GM, Montefiori DC, Kepler TB, Tomaras GD, Alam SM, Liao H-X, Haynes BF. 2011. Analysis of a clonal lineage of HIV-1 envelope V2/V3 conformational epitope-specific broadly neutralizing antibodies and their inferred unmutated common ancestors. J Virol 85:9998–10009. https://doi.org/10.1128/JVI.05045-11.
61. Cardoso RMF, Brunel FM, Ferguson S, Zwick M, Burton DR, Dawson PE, Wilson IA. 2007. Structural basis of enhanced binding of extended and helically constrained peptide epitopes of the broadly neutralizing HIV-1 antibody 4E10. J Mol Biol 365:1533–1544. https://doi.org/10.1016/j.jmb.2006.10.088.
62. Pancera M, McLellan JS, Wu X, Zhu J, Changela A, Schmidt SD, Yang Y, Zhou T, Phogat S, Mascola JR, Kwong PD. 2010. Crystal structure of PG16 and chimeric dissection with somatically related PG9: structure-function analysis of two quaternary-specific antibodies that effectively neutralize HIV-1. J Virol 84:8098–8110. https://doi.org/10.1128/JVI.00966-10.
63. Huang J, Ofek G, Laub L, Louder MK, Doria-Rose NA, Longo NS, Imamichi H, Bailer RT, Chakrabarti B, Sharma SK, Alam SM, Wang T, Yang Y, Zhang B, Migueles SA, Wyatt R, Haynes BF, Kwong PD, Mascola JR, Connors M. 2012. Broad and potent neutralization of HIV-1 by a gp41-specific human antibody. Nature 491:406–412. https://doi.org/10.1038/nature11544.
64. Julien JP, Sok D, Khayat R, Lee JH, Doores KJ, Walker LM, Ramos A, Diwanji DC, Pejchal R, Cupo A, Katpally U, Depetris RS, Stanfield RL, McBride R, Marozsan AJ, Paulson JC, Sanders RW, Moore JP, Burton DR, Poignard P, Ward AB, Wilson IA. 2013. Broadly neutralizing antibody PGT121 allosterically modulates CD4 binding via recognition of the HIV-1 gp120 V3 base and multiple surrounding glycans. PLoS Pathog 9:e1003342. https://doi.org/10.1371/journal.ppat.1003342.
65. Barbas CF, Collet TA, Amberg W, Roben P, Binley JM, Hoekstra D, Cababa D, Jones TM, Williamson RA, Pilkington GR, Haigwood NL, Cabezas E, Satterthwait AC, Sanz I, Burton DR. 1993. Molecular profile of an antibody response to HIV-1 as probed by combinatorial libraries. J Mol Biol 230:812–823. https://doi.org/10.1006/jmbi.1993.1203.
66. Doores KJ, Kong L, Krumm SA, Le KM, Sok D, Laserson U, Garces F, Poignard P, Wilson IA, Burton DR. 2015. Two classes of broadly neutralizing antibodies within a single lineage directed to the high-mannose patch of HIV envelope. J Virol 89:1105–1118. https://doi.org/10.1128/JVI.02905-14.
67. Montgomery DL, Wang YJ, Hrin R, Luftig M, Su B, Miller MD, Wang F, Haytko P, Huang L, Vitelli S, Condra J, Liu X, Hampton R, Carfi A, Pessi A, Bianchi E, Joyce J, Lloyd C, Geleziunas R, Bramhill D, King VM, Finnefrock AC, Strohl W, An Z. 2009. Affinity maturation and characterization of a human monoclonal antibody against HIV-1 gp41. MAbs 1:462–474. https://doi.org/10.4161/mabs.1.5.9214.
68. E De R, Vassell R, Wingfield PT, Wild CT, Weiss CD. 2001. Peptides corresponding to the heptad repeat motifs in the transmembrane protein (gp41) of human immunodeficiency virus type 1 elicit antibodies to receptor-activated conformations of the envelope glycoprotein. J Virol 75:8859–8863. https://doi.org/10.1128/jvi.75.18.8859-8863.2001.
69. Bianchi E, Joyce JG, Miller MD, Finnefrock AC, Liang X, Finotto M, Ingallinella P, Mckenna P, Citron M, Ottinger E, Hepler RW, Hrin R, Nahas D, Wu C, Montefiori D, Shiver JW, Pessi A, Kim PS. 2010. Vaccination with peptide mimetics of the gp41 prehairpin fusion intermediate yields neutralizing antisera against HIV-1 isolates. Proc Natl Acad Sci U S A 107:10655–10660. https://doi.org/10.1073/pnas.1004261107.
70. Qi Z, Pan C, Lu H, Shui Y, Li L, Li X, Xu X, Liu S, Jiang S. 2010. A recombinant mimetics of the HIV-1 gp41 prehairpin fusion intermediate fused with human IgG Fc fragment elicits neutralizing antibody response in the vaccinated mice. Biochem Biophys Res Commun 398:506–512. https://doi.org/10.1016/j.bbrc.2010.06.109.
71. Montefiori DC, Filsinger Interrante MV, Bell BN, Rubio AA, Joyce JG, Shiver JW, LaBranche CC, Kim PS. 2021. The high-affinity immunoglobulin receptor FcγRI potentiates HIV-1 neutralization via antibodies against the gp41 N-heptad repeat. Proc Natl Acad Sci U S A 118:e2018027118. https://doi.org/10.1073/pnas.2018027118.
72. Perez LG, Costa MR, Todd CA, Haynes BF, Montefiori DC. 2009. Utilization of immunoglobulin G Fc receptors by human immunodeficiency virus type 1: a specific role for antibodies against the membrane-proximal external region of gp41. J Virol 83:7397–7410. https://doi.org/10.1128/JVI.00656-09.
73. Perez LG, Zolla-Pazner S, Montefiori DC. 2013. Antibody-dependent, FcγRI-mediated neutralization of HIV-1 in TZM-bl cells occurs independently of phagocytosis. J Virol 87:5287–5290. https://doi.org/10.1128/JVI.00278-13.
74. Todd CA, Greene KM, Yu X, Ozaki DA, Gao H, Huang Y, Wang M, Li G, Brown R, Wood B, D'Souza MP, Gilbert P, Montefiori DC, Sarzotti-Kelsoe M. 2012. Development and implementation of an international proficiency testing program for a neutralizing antibody assay for HIV-1 in TZM-bl cells. J Immunol Methods 375:57–67. https://doi.org/10.1016/j.jim.2011.09.007.
75. Sarzotti-Kelsoe M, Bailer RT, Turk E, Lin C, Bilska M, Greene KM, Gao H, Todd CA, Ozaki DA, Seaman MS, Mascola JR, Montefiori DC. 2014. Optimization and validation of the TZM-bl assay for standardized assessments of neutralizing antibodies against HIV-1. J Immunol Methods 409:131–146. https://doi.org/10.1016/j.jim.2013.11.022.
76. Mascola JR, D'Souza P, Gilbert P, Hahn BH, Haigwood NL, Morris L, Petropoulos CJ, Polonis VR, Sarzotti M, Montefiori DC. 2005. Recommendations for the design and use of standard virus panels to assess neutralizing antibody responses elicited by candidate human immunodeficiency virus type 1 vaccines. J Virol 79:10103–10107. https://doi.org/10.1128/JVI.79.16.10103-10107.2005.
77. DeCamp A, Hraber P, Bailer RT, Seaman MS, Ochsenbauer C, Kappes J, Gottardo R, Edlefsen P, Self S, Tang H, Greene K, Gao H, Daniell X, Sarzotti-Kelsoe M, Gorny MK, Zolla-Pazner S, LaBranche CC, Mascola JR, Korber BT, Montefiori DC. 2014. Global panel of HIV-1 Env reference strains for standardized assessments of vaccine-elicited neutralizing antibodies. J Virol 88:2489–2507. https://doi.org/10.1128/JVI.02853-13.

78. Montefiori DC. 2009. Measuring HIV neutralization in a luciferase reporter gene assay, p 395–405. *In* Prasad VR, Kalpana GV (ed), HIV protocols, 2nd ed. Humana Press, Totowa, NJ.
79. Bianchi E, Finotto M, Ingallinella P, Hrin R, Carella AV, Hou XS, Schleif WA, Miller MD, Geleziunas R, Pessi A. 2005. Covalent stabilization of coiled coils of the HIV gp41 N region yields extremely potent and broad inhibitors of viral infection. Proc Natl Acad Sci U S A 102:12903–12908. https://doi.org/10.1073/pnas.0502449102.
80. Eckert DM, Shi Y, Kim S, Welch BD, Kang E, Poff ES, Kay MS. 2008. Characterization of the steric defense of the HIV-1 gp41 N-trimer region. Protein Sci 17:2091–2100. https://doi.org/10.1110/ps.038273.108.
81. Hamburger AE, Kim S, Welch BD, Kay MS. 2005. Steric accessibility of the HIV-1 gp41 N-trimer region. J Biol Chem 280:12567–12572. https://doi.org/10.1074/jbc.M412770200.
82. Lu L, Wei M, Chen Y, Xiong W, Yu F, Qi Z, Jiang S, Pan C. 2013. F(ab′)2 fragment of a gp41 NHR-trimer-induced IgM monoclonal antibody neutralizes HIV-1 infection and blocks viral fusion by targeting the conserved gp41 pocket. Microbes Infect 15:887–894. https://doi.org/10.1016/j.micinf.2013.10.001.
83. Robertson D, Anderson J, Bradac J, Carr J, Foley B, Funkhouser R, Gao F, Hahn B, Kalish M, Kuiken C, Learn G, Leitner T, McCutchan F, Osmanov S, Peeters M, Pieniazek D, Salminen M, Sharp P, Wolinsky S, Korber B. 2000. HIV-1 nomenclature proposal. Science 288:55. https://doi.org/10.1126/science.288.5463.55d.
84. Li M, Gao F, Mascola JR, Stamatatos L, Polonis VR, Koutsoukos M, Voss G, Goepfert P, Gilbert P, Greene KM, Bilska M, Kothe DL, Salazar-Gonzalez JF, Wei X, Decker JM, Hahn BH, Montefiori DC. 2005. Human immunodeficiency virus type 1 *env* clones from acute and early subtype B infections for standardized assessments of vaccine-elicited neutralizing antibodies. J Virol 79:10108–10125. https://doi.org/10.1128/JVI.79.16.10108-10125.2005.
85. Li M, Salazar-Gonzalez JF, Derdeyn CA, Morris L, Williamson C, Robinson JE, Decker JM, Li Y, Salazar MG, Polonis VR, Mlisana K, Karim SA, Hong K, Greene KM, Bilska M, Zhou J, Allen S, Chomba E, Mulenga J, Vwalika C, Gao F, Zhang M, Korber BTM, Hunter E, Hahn BH, Montefiori DC. 2006. Genetic and neutralization properties of subtype C human immunodeficiency virus type 1 molecular *env* clones from acute and early heterosexually acquired infections in Southern Africa. JVI 80:11776–11790. https://doi.org/10.1128/JVI.01730-06.
86. Shang H, Han X, Shi X, Zuo T, Goldin M, Chen D, Han B, Sun W, Wu H, Wang X, Zhang L. 2011. Genetic and neutralization sensitivity of diverse HIV-1 env clones from chronically infected patients in China. J Biol Chem 286:14531–14541. https://doi.org/10.1074/jbc.M111.224527.
87. Revilla A, Delgado E, Christian EC, Dalrymple J, Vega Y, Carrera C, González-Galeano M, Ocampo A, De Castro RO, Lezaún MJ, Rodríguez R, Mariño A, Ordóñez P, Cilla G, Cisterna R, Santamaría JM, Prieto S, Rakhmanova A, Vinogradova A, Ríos M, Pérez-Álvarez L, Nájera R, Montefiori DC, Seaman MS, Thomson MM. 2011. Construction and phenotypic characterization of HIV type 1 functional envelope clones of subtypes G and F. AIDS Res Hum Retroviruses 27:889–901. https://doi.org/10.1089/aid.2010.0177.
88. Kulkarni SS, Lapedes A, Tang H, Gnanakaran S, Daniels MG, Zhang M, Bhattacharya T, Li M, Polonis VR, McCutchan FE, Morris L, Ellenberger D, Butera ST, Bollinger RC, Korber BT, Paranjape RS, Montefiori DC. 2009. Highly complex neutralization determinants on a monophyletic lineage of newly transmitted subtype C HIV-1 Env clones from India. Virology 385:505–520. https://doi.org/10.1016/j.virol.2008.12.032.
89. Li Y, Migueles SA, Welcher B, Svehla K, Phogat A, Louder MK, Wu X, Shaw GM, Connors M, Wyatt RT, Mascola JR. 2007. Broad HIV-1 neutralization mediated by CD4-binding site antibodies. Nat Med 13:1032–1034. https://doi.org/10.1038/nm1624.
90. Seaman MS, Janes H, Hawkins N, Grandpre LE, Devoy C, Giri A, Coffey RT, Harris L, Wood B, Daniels MG, Bhattacharya T, Lapedes A, Polonis VR, McCutchan FE, Gilbert PB, Self SG, Korber BT, Montefiori DC, Mascola JR. 2010. Tiered categorization of a diverse panel of HIV-1 Env pseudoviruses for assessment of neutralizing antibodies. J Virol 84:1439–1452. https://doi.org/10.1128/JVI.02108-09.
91. Page KA, Landau NR, Littman DR. 1990. Construction and use of a human immunodeficiency virus vector for analysis of virus infectivity. J Virol 64:5270–5276. https://doi.org/10.1128/JVI.64.11.5270-5276.1990.
92. Li Y, Svehla K, Mathy NL, Voss G, Mascola JR, Wyatt R. 2006. Characterization of antibody responses elicited by human immunodeficiency virus type 1 primary isolate trimeric and monomeric envelope glycoproteins in selected adjuvants. J Virol 80:1414–1426. https://doi.org/10.1128/JVI.80.3.1414-1426.2006.
93. Long EM, Rainwater SMJ, Lavreys L, Mandaliya K, Overbaugh J. 2002. HIV type 1 variants transmitted to women in Kenya require the CCR5 coreceptor for entry, regardless of the genetic complexity of the infecting virus. AIDS Res Hum Retroviruses 18:567–576. https://doi.org/10.1089/088922202753747914.
94. Cheng-Mayer C, Liu R, Landau NR, Stamatatos L. 1997. Macrophage tropism of human immunodeficiency virus type 1 and utilization of the CC-CKR5 coreceptor. J Virol 71:1657–1661. https://doi.org/10.1128/JVI.71.2.1657-1661.1997.
95. Stamatatos L, Lim M, Cheng-Mayer C. 2000. Generation and structural analysis of soluble oligomeric gp140 envelope proteins derived from neutralization-resistant and neutralization-susceptible primary HIV type 1 isolates. AIDS Res Hum Retroviruses 16:981–994. https://doi.org/10.1089/08892220050058407.
96. Stamatatos L, Wiskerchen M, Cheng-Mayer C. 1998. Effect of major deletions in the V1 and V2 loops of a macrophage-tropic HIV type 1 isolate on viral envelope structure, cell entry, and replication. AIDS Res Hum Retroviruses 14:1129–1139. https://doi.org/10.1089/aid.1998.14.1129.
97. Gao F, Morrison SG, Robertson DL, Thornton CL, Craig S, Karlsson G, Sodroski J, Morgado M, Galvao-Castro B, Von Briesen H, Beddows S, Weber J, Sharp PM, Shaw GM, Hahn BH. 1996. Molecular cloning and analysis of functional envelope genes from human immunodeficiency virus type 1 sequence subtypes A through G. J Virol 70:1651–1667. https://doi.org/10.1128/JVI.70.3.1651-1667.1996.
98. Poss M, Overbaugh J. 1999. Variants from the diverse virus population identified at seroconversion of a clade A human immunodeficiency virus type 1-infected woman have distinct biological properties. J Virol 73:5255–5264. https://doi.org/10.1128/JVI.73.7.5255-5264.1999.
99. Bruhns P, Iannascoli B, England P, Mancardi DA, Fernandez N, Jorieux S, Daëron M. 2009. Specificity and affinity of human Fcγ receptors and their polymorphic variants for human IgG subclasses. Blood 113:3716–3725. https://doi.org/10.1182/blood-2008-09-179754.
100. van der Poel CE, Spaapen RM, van de Winkel JGJ, Leusen JHW. 2011. Functional Characteristics of the High Affinity IgG Receptor, FcγRI. J Immunol 186:2699–2704. https://doi.org/10.4049/jimmunol.1003526.
101. Montero M, van Houten NE, Wang X, Scott JK. 2008. The membrane-proximal external region of the human immunodeficiency virus type 1 envelope: dominant site of antibody neutralization and target for vaccine design. Microbiol Mol Biol Rev 72:54–84. https://doi.org/10.1128/MMBR.00020-07.
102. Gach JS, Leaman DP, Zwick MB. 2011. Targeting HIV-1 gp41 in close proximity to the membrane using antibody and other molecules. Curr Top Med Chem 11:2997–3021. https://doi.org/10.2174/156802611798808505.
103. Patterson S, Rae A, Hockey N, Gilmour J, Gotch F. 2001. Plasmacytoid dendritic cells are highly susceptible to human immunodeficiency virus type 1 infection and release infectious virus. J Virol 75:6710–6713. https://doi.org/10.1128/JVI.75.14.6710-6713.2001.
104. Shen R, Richter HE, Clements RH, Novak L, Huff K, Bimczok D, Sankaran-Walters S, Dandekar S, Clapham PR, Smythies LE, Smith PD. 2009. Macrophages in vaginal but not intestinal mucosa are monocyte-like and permissive to human immunodeficiency virus type 1 infection. J Virol 83:3258–3267. https://doi.org/10.1128/JVI.01796-08.
105. Kruize Z, Kootstra NA. 2019. The role of macrophages in HIV-1 persistence and pathogenesis. Front Microbiol 10:2828. https://doi.org/10.3389/fmicb.2019.02828.
106. Smed-Sörensen A, Loré K, Vasudevan J, Louder MK, Andersson J, Mascola JR, Spetz A-L, Koup RA. 2005. Differential susceptibility to human immunodeficiency virus type 1 infection of myeloid and plasmacytoid dendritic cells. J Virol 79:8861–8869. https://doi.org/10.1128/JVI.79.14.8861-8869.2005.
107. Loré K, Smed-Sörensen A, Vasudevan J, Mascola JR, Koup RA. 2005. Myeloid and plasmacytoid dendritic cells transfer HIV-1 preferentially to antigen-specific $CD4^+$ T cells. J Exp Med 201:2023–2033. https://doi.org/10.1084/jem.20042413.
108. Groot F, Welsch S, Sattentau QJ. 2008. Efficient HIV-1 transmission from macrophages to T cells across transient virological synapses. Blood 111:4660–4663. https://doi.org/10.1182/blood-2007-12-130070.
109. Waki K, Freed EO. 2010. Macrophages and cell-cell spread of HIV-1. Viruses 2:1603–1620. https://doi.org/10.3390/v2081603.
110. Bracq L, Xie M, Benichou S, Bouchet J. 2018. Mechanisms for cell-to-cell transmission of HIV-1. Front Immunol 9:260. https://doi.org/10.3389/fimmu.2018.00260.

111. Spira AI, Marx PA, Patterson BK, Mahoney J, Koup A, Wolinsky SM, Ho DD. 1996. Cellular targets of infection and route of viral dissemination after an intravaginal inoculation of simian immunodeficiency virus into rhesus macaques. J Exp Med 183:215–225. https://doi.org/10.1084/jem.183.1.215.
112. Hu J, Gardner MB, Miller CJ. 2000. Simian immunodeficiency virus rapidly penetrates the cervicovaginal mucosa after intravaginal inoculation and infects intraepithelial dendritic cells. J Virol 74:6087–6095. https://doi.org/10.1128/jvi.74.13.6087-6095.2000.
113. Pope M, Haase AT. 2003. Transmission, acute HIV-1 infection and the quest for strategies to prevent infection. Nat Med 9:847–852. https://doi.org/10.1038/nm0703-847.
114. Su B, Dispinseri S, Iannone V, Zhang T, Wu H, Carapito R, Bahram S, Scarlatti G, Moog C. 2019. Update on Fc-mediated antibody functions against HIV-1 beyond neutralization. Front Immunol 10:2968. https://doi.org/10.3389/fimmu.2019.02968.
115. Stieh DJ, Maric D, Kelley ZL, Anderson MR, Hattaway HZ, Beilfuss BA, Rothwangl KB, Veazey RS, Hope TJ. 2014. Vaginal challenge with an SIV-based dual reporter system reveals that infection can occur throughout the upper and lower female reproductive tract. PLoS Pathog 10:e1004440. https://doi.org/10.1371/journal.ppat.1004440.
116. Stieh DJ, Matias E, Xu H, Fought AJ, Blanchard JL, Marx PA, Veazey RS, Hope TJ. 2016. Th17 cells are preferentially infected very early after vaginal transmission of SIV in macaques. Cell Host Microbe 19:529–540. https://doi.org/10.1016/j.chom.2016.03.005.
117. Klein K, Veazey RS, Warrier R, Hraber P, Doyle-Meyers LA, Buffa V, Liao H-X, Haynes BF, Shaw GM, Shattock RJ. 2013. Neutralizing IgG at the portal of infection mediates protection against vaginal simian/human immunodeficiency virus challenge. J Virol 87:11604–11616. https://doi.org/10.1128/JVI.01361-13.
118. Hessell AJ, Rakasz EG, Tehrani DM, Huber M, Weisgrau KL, Landucci G, Forthal DN, Koff WC, Poignard P, Watkins DI, Burton DR. 2010. Broadly neutralizing monoclonal antibodies 2F5 and 4E10 directed against the human immunodeficiency virus type 1 gp41 membrane-proximal external region protect against mucosal challenge by simian-human immunodeficiency virus SHIVBa-L. J Virol 84:1302–1313. https://doi.org/10.1128/JVI.01272-09.
119. Pegu A, Yang ZY, Boyington JC, Wu L, Ko SY, Schmidt SD, McKee K, Kong WP, Shi W, Chen X, Todd JP, Letvin NL, Huang J, Nason MC, Hoxie JA, Kwong PD, Connors M, Rao SS, Mascola JR, Nabel GJ. 2014. Neutralizing antibodies to HIV-1 envelope protect more effectively in vivo than those to the CD4 receptor. Sci Transl Med 6:243ra88. https://doi.org/10.1126/scitranslmed.3008992.
120. Pegu A, Borate B, Huang Y, Pauthner MG, Hessell AJ, Julg B, Doria-Rose NA, Schmidt SD, Carpp LN, Cully MD, Chen X, Shaw GM, Barouch DH, Haigwood NL, Corey L, Burton DR, Roederer M, Gilbert PB, Mascola JR, Huang Y. 2019. A meta-analysis of passive immunization studies shows that serum-neutralizing antibody titer associates with protection against SHIV challenge. Cell Host Microbe 26:336–346. https://doi.org/10.1016/j.chom.2019.08.014.
121. Burton DR. 2021. A new lease on life for an HIV-neutralizing antibody class and vaccine target. Proc Natl Acad Sci U S A 118:e2026390118. https://doi.org/10.1073/pnas.2026390118.
122. Barouch DH, Yang Z, Kong W, Korioth-Schmitz B, Sumida SM, Truitt DM, Kishko MG, Arthur JC, Miura A, Mascola JR, Letvin NL, Nabel GJ. 2005. A human T-cell leukemia virus type 1 regulatory element enhances the immunogenicity of human immunodeficiency virus type 1 DNA vaccines in mice and nonhuman primates. J Virol 79:8828–8834. https://doi.org/10.1128/JVI.79.14.8828-8834.2005.
123. Graham FL, Van der Eb AJ. 1973. A new technique for the assay of infectivity of human adenovirus 5 DNA. Virology 52:456–467. https://doi.org/10.1016/0042-6822(73)90341-3.
124. Kutner RH, Zhang XY, Reiser J. 2009. Production, concentration and titration of pseudotyped HIV-1-based lentiviral vectors. Nat Protoc 4:495–505. https://doi.org/10.1038/nprot.2009.22.
125. Pear WS, Nolan GP, Scott ML, Baltimore D. 1993. Production of high-titer helper-free retroviruses by transient transfection. Proc Natl Acad Sci U S A 90:8392–8396. https://doi.org/10.1073/pnas.90.18.8392.
126. Wei X, Decker JM, Liu H, Zhang Z, Arani RB, Kilby JM, Saag MS, Wu X, Shaw GM, Kappes JC. 2002. Emergence of resistant human immunodeficiency virus type 1 in patients receiving fusion inhibitor (T-20) monotherapy. Antimicrob Agents Chemother 46:1896–1905. https://doi.org/10.1128/aac.46.6.1896-1905.2002.
127. Wei X, Decker JM, Wang S, Hui H, Kappes JC, Wu X, Salazar-Gonzalez JF, Salazar MG, Kilby JM, Saag MS, Komarova NL, Nowak MA, Hahn BH, Kwong PD, Shaw GM. 2003. Antibody neutralization and escape by HIV-1. Nature 422:307–312. https://doi.org/10.1038/nature01470.
128. Platt EJ, Wehrly K, Kuhmann SE, Chesebro B, Kabat D. 1998. Effects of CCR5 and CD4 cell surface concentrations on infections by macrophagetropic isolates of human immunodeficiency virus type 1. J Virol 72:2855–2864. https://doi.org/10.1128/JVI.72.4.2855-2864.1998.
129. Derdeyn CA, Decker JM, Sfakianos JN, Wu X, O'Brien WA, Ratner L, Kappes JC, Shaw GM, Hunter E. 2000. Sensitivity of human immunodeficiency virus type 1 to the fusion inhibitor T-20 is modulated by coreceptor specificity defined by the V3 loop of gp120. J Virol 74:8358–8367. https://doi.org/10.1128/jvi.74.18.8358-8367.2000.
130. Takeuchi Y, McClure MO, Pizzato M. 2008. Identification of gammaretroviruses constitutively released from cell lines used for human immunodeficiency virus research. J Virol 82:12585–12588. https://doi.org/10.1128/JVI.01726-08.
131. Platt EJ, Bilska M, Kozak SL, Kabat D, Montefiori DC. 2009. Evidence that ecotropic murine leukemia virus contamination in TZM-bl cells does not affect the outcome of neutralizing antibody assays with human immunodeficiency virus type 1. J Virol 83:8289–8292. https://doi.org/10.1128/JVI.00709-09.
132. Ozaki DA, Gao H, Todd CA, Greene KM, Montefiori DC, Sarzotti-Kelsoe M. 2012. International technology transfer of a GCLP-compliant HIV-1 neutralizing antibody assay for human clinical trials. PLoS One 7:e30963. https://doi.org/10.1371/journal.pone.0030963.